

Alma Mater Studiorum Università di Bologna
Archivio istituzionale della ricerca

Validation of a database of mean uranium, thorium and potassium concentrations in rock samples of Portuguese geological units, generated of literature data

This is the final peer-reviewed author's accepted manuscript (postprint) of the following publication:

Published Version:

Domingos, F., Cinelli, G., Neves, L., Pereira, A., Braga, R., Bossew, P., et al. (2020). Validation of a database of mean uranium, thorium and potassium concentrations in rock samples of Portuguese geological units, generated of literature data. JOURNAL OF ENVIRONMENTAL RADIOACTIVITY, 222, 1-10 [10.1016/j.jenvrad.2020.106338].

Availability:

This version is available at: <https://hdl.handle.net/11585/769988> since: 2020-09-02

Published:

DOI: <http://doi.org/10.1016/j.jenvrad.2020.106338>

Terms of use:

Some rights reserved. The terms and conditions for the reuse of this version of the manuscript are specified in the publishing policy. For all terms of use and more information see the publisher's website.

This item was downloaded from IRIS Università di Bologna (<https://cris.unibo.it/>).
When citing, please refer to the published version.

(Article begins on next page)

This is the final peer-reviewed accepted manuscript of:

Domingos, F., Cinelli, G., Neves, L., Pereira, A., Braga, R., Bossew, P., & Tollefsen, T. (2020). Validation of a database of mean uranium, thorium and potassium concentrations in rock samples of portuguese geological units, generated of literature data. Journal of Environmental Radioactivity, 222

The final published version is available online at
<https://dx.doi.org/10.1016/j.jenvrad.2020.106338>

Rights / License:

The terms and conditions for the reuse of this version of the manuscript are specified in the publishing policy. For all terms of use and more information see the publisher's website.

This item was downloaded from IRIS Università di Bologna (<https://cris.unibo.it/>)

When citing, please refer to the published version.

Validation of a database of mean uranium, thorium and potassium concentrations in rock samples of Portuguese geological units, generated of literature data

Filipa Domingos^{a*}, Giorgia Cinelli^b, Luís Neves^a, Alcides Pereira^a, Roberto Braga^c, Peter Bossew^d, Tore Tollefsen^b

a – CITEUC, Department of Earth Sciences, University of Coimbra, Rua Sílvio Lima, 3030-790, Coimbra.

b - European Commission, DG Joint Research Centre – JRC, Directorate G – Nuclear Safety & Security, Unit G.10 – Knowledge for Nuclear Safety, Security & Safeguards, Radioactivity Environmental Monitoring, Ispra, Italy

c - Dipartimento di Scienze Biologiche, Geologiche e Ambientali (BiGeA), University of Bologna, Piazza di Porta San Donato 1, Bologna, Italy

d - German Federal Office for Radiation Protection, Köpenicker Allee 120-130, 10318 Berlin, Germany

*Corresponding author, e-mail: lipa_domingos@hotmail.com

Highlights

- A database of U, Th and K concentrations in rocks of Portugal established;
- Mean U, Th and K concentrations in rock per geological unit calculated;
- Validation by comparison of calculated to measured mean terrestrial dose rate;
- Investigation of variance components traceable to the geochemical analysis;
- Use of scattered local geochemical data to establish large scale maps enabled.

Abstract

The European Atlas of Natural Radiation has been under development for the past 15 years. Among the lacunae of the Atlas are maps of U, Th and K concentrations in rocks due to lack of European-wide geochemical surveys of bedrock units. The objective of this paper is to investigate the usability of scattered geochemical data of rock samples for large-scale mapping of U, Th and K concentrations in geological units. For this purpose, geochemical data were compiled from grey literature sources to produce a geochemical database (LIT database) that includes 2817 results of U, Th and K concentrations measured in rock samples.

Given the methodical heterogeneity within LIT database, the influence of the geochemical analysis techniques was assessed through a three-way analysis of variance (ANOVA) using geological units, geochemical analysis techniques and loss on ignition (LOI) as categorical variables. The percentage of variation explained by geological factors was 53 % for U, 38 % for Th, 50% for K and 51 % for the terrestrial gamma dose rate (TGDR), while the percentage of variation explained by the geochemical analysis techniques and LOI was generally lower than 5 %. The geological factors were thereby the main source of variability in the data, followed by the error component which can be assumed to represent true spatial variability of geochemical concentrations, hence, variability within the geological units. The reliability of LIT database between the different geochemical analysis techniques was investigated through pairwise comparison of the least square (LS) means computed through the three-way ANOVA for each geochemical analysis technique. The results show an agreement of the LS means between the different geochemical analysis techniques, which indicates that LIT database can be considered consistent within itself, thus, reliable.

In order to validate the usability of literature data, the TGDR calculated from literature data ($TGDR_{calc}$) was compared to the measured TGDR ($TGDR_{obs}$) displayed in the

Radiometric Map of Portugal (RMP) using geological units as reference units. The correlation between $TGDR_{calc}$ and $TGDR_{obs}$ was highly significant ($p < 0.001$) and the results of a paired sample t-test and Wilcoxon median tests indicate that the differences between the arithmetic means of $TGDR_{calc}$ and $TGDR_{obs}$ were not statistically significant ($p = 0.126$ and $p = 0.14$, respectively). Distributions of $TGDR_{calc}$ and $TGDR_{obs}$ are seemingly equal according to the Kolmogorov-Smirnov and Anderson-Darling tests. The pooled standard deviation (SD) of the RMP dataset was set as criterion to assess the discrepancy between the arithmetic means of the RMP and LIT databases. About 14 out of 26 geological units are located within one pooled SD around $TGDR_{obs}$ and only 1 out of 26 units is located outside 2 pooled SDs. Systematic discrepancies were observed for sedimentary rocks possibly due to the lack of representativeness of the data. Nonetheless, the compatibility of the RMP and LIT databases can be considered acceptable, which implies that the estimation of the contents of terrestrial radionuclides using literature data for large-scale mapping of U, Th and K contents in geological units is reasonable.

Keywords: Data compilation; Geochemical analysis techniques; Terrestrial radionuclides; Terrestrial gamma dose rate; Geological units.

1. Introduction

1.1 Motivation

A long-term European project, under way for about 15 years, is the European Atlas of Natural Radiation, of which web and printed versions exist (Cinelli et al., 2019; EC, 2019). The Atlas is however incomplete, as certain compartments and environmental media are missing or fragmentary due to lack of data. Among these lacunae are maps of concentrations of naturally occurring radionuclides, namely isotopes of U, Th and K, in rock. While Europe-wide geochemical surveys of *agricultural and pasture soil* including these radionuclides exist (FOREGS and GEMAS, maps and references in the Atlas), literature data of U, Th and K in *rock* are scattered and methodically highly

heterogeneous. Therefore, creating Europe-wide maps from such data appeared questionable. The alternative, on the other hand, namely creating a methodically homogeneous geochemical database of European rocks from scratch, would pose a tremendous task which is beyond realistic feasibility. Therefore, it has been concluded by the board of experts of the Atlas (to which the authors of this paper belong) to explore the feasibility of maps of U, Th and K concentrations in rocks, derived from literature data. This requires, as very first step, to investigate whether literature data can be used to this end, observing standards of accuracy and precision, given methodical heterogeneity. The objective of this paper is thus, investigating the usability of scattered geochemical literature data for large-scale (in perspective, European scale) mapping. As test region for this study we use the territory of Portugal and as geochemical data sources, local studies on rock geochemistry performed in Portugal.

1.2 Geochemical surveys

Local surveys of geochemistry are profusely available in scientific literature. Large scale surveys are, however, scarce because the generation of a truly representative sample of the media is difficult with limited resources, and sampling of the entire population of landscape units is impractical and costly.

UNESCO initiated the first attempt to create a geochemical map of the world in 1988 through the International Geochemical Mapping Project (IGCP 259) (Xuejing and Hangxin, 2001). The main goal of the project was to estimate the concentration of several elements at a global scale with particular focus on ore pathfinders and radioelements (Darnley 1995, Darnley et al. 1995, Xuejing and Hangxin, 2001). The project intended to overcome the lack of numerical equivalence between compiled datasets that are subject to different sampling and analytical techniques as well as different levels of quality control (Darnley et al. 1995). However, the compilation and normalization of existing datasets required that data at multiple spatial scales be interlinked (Darnley 1995, Darnley et al. 1995).

A compilation of geochemical data hardly fulfills the assumptions of statistical inference (ex. the sampling must be random, unbiased and designed to adequately represent the population, Crumbling, 2001; Ramsey and Hewitt, 2005) as the data have been acquired for different purposes, at different scales and with different methods. However, every geochemical survey must rely on a suitable knowledge of the geology of the surveyed area (e.g. Rollinson, 1993). Thus, geochemical surveys can be presumed to be representative of the geological units sampled.

The estimation of the contents of terrestrial radionuclides, radon, gamma dose rate and air-absorbed dose rate using geochemical data has been attempted at both a local (e.g. Ielsch et al. 2010; Ye and Gan, 2013) and regional scale (e.g. Appleton et al. 2008; Beamish 2014; Ielsch et al. 2017; Marsac et al. 2016). However, the authors often resort to geochemical data available in national databases that have been acquired with consistent analytical techniques and quality control procedures.

1.3 Heterogeneity of literature data

Heterogeneity of literature data occurs on several levels. (1) The data come from regional or local studies of certain rock formations or types with certain geochemical objectives, such as mineral exploration, hydrological investigations etc. While representativeness for the study area can be assumed, it is unclear to which extent this applies to an entire lithological class.

(2) Sampling and sample geo-referencing methods are heterogeneous. For example, many literature sources do not quote locations of individual samples, but only regions of origin. Sometimes, no individual but only aggregated results are given, e.g. arithmetic mean concentrations and standard deviations. This circumstance inhibits the use of geostatistical tools.

(3) Finally, geochemical analytic methodology is heterogeneous. Comparability of results between different studies is therefore not given a priori. Both radiological and geochemical data can be used to evaluate U, Th and K concentrations and distributions

(IAEA, 2010). Radiological data refers to radionuclide concentrations determined through alpha- or gamma-spectrometry while geochemical data may be acquired through various geochemical analysis techniques (hereafter referred to as analytical techniques), such as X-Ray Fluorescence (XRF), Induced Coupled Plasma Spectrometry (ICP) or Instrumental Neutron Activation Analysis (INAA), among others.

It should be stressed again that heterogeneity between studies does not mean to invalidate the individual studies, but it is an obstacle to using them as input for maps beyond the scale of the individual ones. Investigating whether it is still possible, is the subject of this paper.

1.4 Variability of true and measured geochemical concentrations

The idea underlying the analysis performed in this study is that there are essentially three components of variability:

(A) Variability between geological units, leading to variance between geochemical concentrations of samples (or studies, representing aggregated samples) located in different geological units, as this factor is assumed to control geochemical concentration; this component represents *true spatial variability* of the investigated variable (geochemical concentration).

(B) Variance due to different analytical techniques, as it is known that different techniques applied to the same sample, i.e. same true concentration, can lead to systematically different results (e.g. Rollinson, 1993). This component refers to the *observation process* of the variable, not to its true variability over a geological unit.

(C) Variance due to lack of spatial representativeness: assume two studies using same analytical technique, performed in different parts of the same geological unit. Due to true spatial variability within geological units, the results will still be different, in general, in spite of variance sources (1) and (2) excluded. This effect can only be avoided (asymptotically with sample size) if the sample covers the domain (geological unit) representatively. (Representativeness means that the statistical distribution of the sample is asymptotically the same as the true distribution of the investigated variable,

here geochemical concentration.) This component refers to availability of data within a geological unit and their aggregation within and can be understood as sampling effect induced by true variability, component (1). Getting hold of this component is particularly difficult.

1.5 Validation of usability of literature data

The tool to validate the usability of geochemical literature data is comparison of terrestrial gamma dose rate (TGDR) calculated from geochemical concentrations with measured ones. Coincidence within tolerable deviation is a *necessary condition* of the validity of regional estimates from scattered literature data. The strategy is therefore, 1) estimate mean U, Th, K concentrations of geological units from literature data; 2) calculate the mean TGDR per unit and 3) compare these calculated with measured mean TGDR of the same units. This is possible for Portugal as test region, as a fine-grained TGDR map of Portugal is available. If it is proven that creating maps of rock geochemistry from scattered literature data is possible in Portugal, it can plausibly be assumed that this is possible also in other regions.

1.6 Organization of this paper

In the methods section (2), we first establish the geological classification scheme which leads to the set of geological units in which geochemical literature data are aggregated and mean dose rates are calculated. This is followed by a presentation of the compiled geochemical database (section 2.2) and the TGDR map of Portugal (2.3). In section 2.4, the conversion of geochemical concentration into TGDR is reviewed and in 2.5, we explain statistical techniques.

The results section (3) is firstly devoted to analyzing the sources of variance A and B (geology and analytical techniques) in section 3.1. Then an attempt is made to remove source B, to assess the effect of lack of representativeness at least qualitatively (section 3.2). The validation analysis through terrestrial dose rate is shown in section 3.3.

2. Materials and Methods

2.1. Geological classification scheme

OneGeology-Europe (OGE) data were chosen as the geological map to be used as reference because they are available at the European level (at <http://www.onegeology-europe.org/>), providing access to geological maps at the scale of 1:1,000,000 (Baker and Jackson, 2010). The OGE map for Portugal was developed through collaboration with the Portuguese National Laboratory of Energy and Geology (LNEG), and comprises three distinct layers, namely lithology, age and geological structures. The code classification scheme of the OGE map is equivalent to the code classification scheme of the Portuguese Geological Map (PGM) at the scale of 1:1,000,000 published in 2010 by LNEG, and available at <http://geoportal.lneg.pt/geoportal/mapas/index.html>. The OGE classification comprises 76 geological units in mainland Portugal and 11 units in the Madeira and Azores archipelagos. A summary description of the geological units studied in the present work is presented in Table 1 according to Baker and Jackson (2010). A simplified geological map is presented in Figure 1a.

2.2. The Radiometric Map of Portugal

The Radiometric Map of Portugal (RMP, Figure 1b, Batista et al. 2013) displays the terrestrial gamma dose rate in mainland Portugal and is further denoted as $TGDR_{obs}$. A raster layer is available freely at <http://geoportal.lneg.pt/geoportal/mapas/index.html>. The data were acquired with hand-carried, vehicle-borne and air-borne equipment from 1955 onwards (Batista et al. 2012). The equipment used were calibrated either using sources of terrestrial radionuclides with known concentrations of U, Th and K or by measuring the same sites with different equipment (Batista et al. 2012; Grasty et al. 1993). The first radiometric maps of Portugal were produced based on 733,201 measurement points by linear interpolation with the minimum curvature method. The estimation grid consists of 250 m × 250 m cells. A minimum of 10 measurement points was defined necessary for estimation on each grid point, to assure reasonable statistical reliability. This required a search radius of 10 km around every grid point to make sure that the required minimum

number of observations could be achieved (Torres et al. 1997; Saraiva et al. 1998). The updated RMP was produced based on 841,440 measurement points following the acquisition of new data to fill the gaps in the previously developed maps (Batista et al. 2012; Batista et al. 2013).

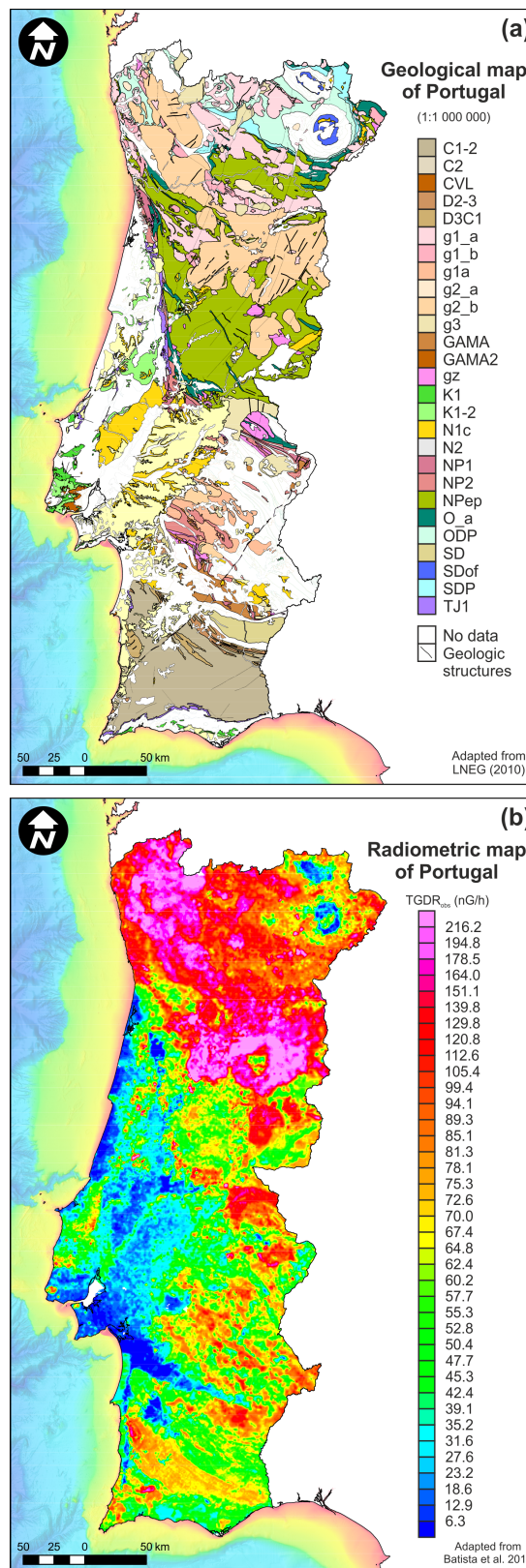
The cell size of the RMP constitutes an important limitation for geological units that have a large perimeter to area ratio, such as vein-type rocks (perimeter to area ratio generally higher than 5). The width of the f1 and f2 (basic vein-type rocks) and qz (quartz veins) units is generally lower than 500 m. Given the RMP cell size of 250 m and the search radius of 10 km used to reach a minimum of 10 measurement points for interpolation, the $TGDR_{obs}$ for these units is highly influenced by the $TGDR_{obs}$ of neighboring geological units. Therefore, the $TGDR_{obs}$ of vein-type rocks displayed in the RMP is unreliable. For this reason, vein-type geological units were excluded from the analysis. This is unfortunate because these units often contain concentrations of radioactive elements strongly different from their surroundings and should therefore be given particular attention for radioprotection reasons. The methodical alternative would have been a different interpolation scheme for such units, but the original raw TGDR data which would be necessary for this, are not available to us.

The lack of access to the original raw TGDR data inhibits the assessment of the influence of the presence of unconsolidated overburden and soil units in the measured TGDR. However, the RMP was primarily developed for the purpose of mineral exploration (Batista et al. 2012; Grasty et al. 1993, Saraiva et al. 1998; Tauchid and Grasty, 2002; Torres and Grasty, 1993). Sampling was focused on the main geological units, as surveys were carried preferentially over crystalline areas, followed by the Mesozoic and Cenozoic sedimentary basins (Torres and Grasty, 1993). Data from car, foot and air-borne surveys were calibrated through measurement of selected areas of exposed bedrock of the main geological units (Torres and Grasty, 1993). The RMP thus reflects the geological character of Portugal (Batista et al. 2012; Grasty et al. 1993,

218 Saraiva et al. 1998; Tauchid and Grasty, 2002; Torres and Grasty, 1993). Thus, the RMP
219 data can be presumed to be representative of the geological units.

220 **Table 1.** Summary description of the geological units studied according to OGE data
221 (Baker and Johnson, 2010).

Group	OGE unit	Perimeter/Area ratio	Lower age	Upper age	Predominant Lithology	Subordinate lithology
Sedimentary rocks	N2	0.9	Pliocene	Pliocene	Sandstone	Conglomerate, Siltstone
	N1c	1.2	Miocene	Miocene	Sandstone	Conglomerate, Siltstone
	K1-2	1.4	Cretaceous	Cretaceous	Limestone	Sandstone, Impure carbonate sedimentary rock, Dolomite
	K1	1.8	Early/Lower Cretaceous	Early/Lower Cretaceous	Sandstone	Limestone, Impure carbonate sedimentary rock, Dolomite
	TJ1	2.2	Late/Upper Triassic	Middle Jurassic	Sandstone	Claystone, Evaporite, Limestone
	C2	3.6	Pennsylvanian	Pennsylvanian	Conglomerate	Sandstone, Claystone, Coal
Metamorphic rocks	C1-2	0.3	Carboniferous	Carboniferous	Phyllite	-
	D2-3	1.9	Middle Devonian	Late/Upper Devonian	Phyllite	Quartzite
	SDof	1.2	Silurian	Devonian	Amphibolite	Schist, Fine grained igneous rock
	SD	0.4	Silurian	Early/Lower Devonian	Phyllite	-
	SDP	0.7	Ordovician	Devonian	Phyllite	-
	ODP	0.8	Ordovician	Devonian	Quartzite	-
	O_a	1.6	Ordovician	Ordovician	Quartzite	Phyllite
	gz	1.1	Furongian	Middle Ordovician	Orthogneiss	Granite, Diorite
	Npep	0.6	Ediacarian	Cambrian	Phyllite	-
	NP2	1.4	Neoproterozoic	Neoproterozoic	Phyllite	-
	NP1	1.6	Neoproterozoic	Neoproterozoic	Schist	Gneiss, Migmatite
Igneous rocks	GAMA2	3.8	Late/Upper Cretaceous	Late/Upper Cretaceous	Diorite	Gabbro
	CVL	2.2	Late/Upper Cretaceous	Late/Upper Cretaceous	Basalt	Pyroclastic material, Gabbro,
	g1_b	1.1	Pennsylvanian	Cisuralian	Granite	-
	g2_b	0.3	Pennsylvanian	Cisuralian	Granite	-
	g3	0.7	Pennsylvanian	Cisuralian	Granite	-
	g1_a	0.7	Mississippian	Pennsylvanian	Granite	-
	g2_a	0.7	Mississippian	Pennsylvanian	Granite	-
	g1a	0.8	Late/Upper Devonian	Pennsylvanian	Tonalite	Granodiorite,
	GAMA	1.3	Late/Upper Devonian	Pennsylvanian	Gabbro	Anorthositic rock, Diorite
	D3C1	1.4	Late/Upper Devonian	Pennsylvanian	Fine grained igneous rock	Phyllite
*The perimeter to area ratio was computed as the ratio between the sum of the perimeter to the sum of the area of all polygons of the geological unit.						



222

223 **Figure 1. a)** Geological units studied. Adapted from the Geological Map of Portugal at
 224 the scale of 1:1,000,000 (LNEG, 2010). **b)** Radiometric Map of Portugal (Batista et al.
 225 2013). Bathymetry was retrieved from [http://portal.emodnet-bathymetry.eu/mean-depth-](http://portal.emodnet-bathymetry.eu/mean-depth-full-coverage)
 226 full-coverage (last accessed in February 2017).

2.3. The geochemical database

A compilation of geochemical surveys available in mainland Portugal was carried out in order to produce a new geochemical database, called LIT to denote that it consists of literature data. The LIT database includes 2817 observations of U, Th and/or K concentrations measured in rock samples presumed to be representative of the geological units studied. The data included in the LIT database were retrieved from the references listed in table A1 (Supplementary material). All samples included in the LIT database were collected in areas of bedrock exposed on the earth surface excluding data retrieved from Cerejo (2013), Pinto (2014), Oliveira (2015) and Dinis et al. (2011) whom also studied rock samples retrieved from boreholes and/or underground galleries. Due to the inherent modifications caused by in-situ chemical and physical weathering, erosion and transport, among others, soil samples and unconsolidated materials are not considered representative of geological units, hence, were excluded from the analysis. Data for the Azores and Madeira archipelagos were not included in the database as the RMP only covers mainland Portugal (Batista et al. 2013).

Three types of samples were considered as observations: (1) individual analyses of rock samples; (2) analyses of composite samples (mixtures of several individual samples taken within an area, analyzed as one sample; the purpose is to reduce variability) and (3) averages of individual samples' analyses. Statistically, sample averages were treated as individual samples; (3) can be thought as mathematical mixing in analogy to physical mixing in (2). The accurate location of the sampling sites of the observations are mostly unknown inhibiting the use of geostatistical tools. This is because in earlier surveys, georeferencing was not considered necessary. Due to this limitation, the regionalization of the available data was carried out using geological information.

Each observation of the LIT database was classified with a code of the geological classification scheme described in section 2.1. according to the location of the observations or the study area (when provided by the authors), or, in alternative, through

the lithologic, petrographic or paleontological features of the samples. A summary of the data available by geological unit (Table A1) and by analytical techniques (Table A2) are given as supplementary material.

For each observation of U, Th and/or K, the element concentration and analytical techniques were registered as provided by the authors. No corrections to U, Th and/or K concentrations were applied for loss on ignition (LOI) or the volatile content. A binary categorical variable for the computation of the effects of LOI in an Analysis of Variance (ANOVA) was defined. Each observation was classified as “TRUE” if the authors estimated LOI (and/or the volatile content) but did not correct the data for LOI and “FALSE” if the authors estimated and corrected the concentration of terrestrial radionuclides using LOI data.

Values reported as below the lower limit of detection (LLD) as well as zeroes were set to 0.65LLD or to an arbitrary small value in case the LLD was not provided by the authors. The overall percentage of values below the LLD was 6% for U, 4% for Th and less than 1% for K.

2.4 Calculation of terrestrial gamma dose rate TGDR

U, Th and K concentration were converted into activity concentration using appropriate conversion factors (Table 2). The TGDR, further denoted as $TGDR_{calc}$, was computed from U, Th and K activity concentration (in Bq/kg) according to the following equation:

$$TGDR_{calc} = 0.0417 \times {}^{40}K + 0.462 \times {}^{238}U + 0.604 \times {}^{232}Th \quad (1)$$

The dose conversion factors (in Bq/kg) of 0.0417, 0.462 and 0.604 were from UNSCEAR (2010). All observations were considered valid, regardless of the analytical technique used in the analysis, and representative of the geological unit sampled by the authors. The database of U, Th and K contents in activity concentration is presented as Supplementary material (Table B1).

Table 2. Conversion factors.

<i>From</i>	<i>To</i>	<i>Conversion</i>
U (mg/kg)	²³⁸ U (Bq/kg)	²³⁸ U (Bq/kg) = U (mg/kg) x 12.35
U (mg/kg)	²²⁶ Ra (Bq/kg)	²²⁶ Ra (Bq/kg) = U (mg/kg) x 12.35
Th (mg/kg)	²⁰⁸ Tl (Bq/kg)	²⁰⁸ Tl (Bq/kg) = Th (mg/kg) x 4.063
K (%)	⁴⁰ K (Bq/kg)	⁴⁰ K (Bq/kg) = K (%) x 312.5

2.5. Data analysis

a) Influence of analytical techniques

The influence of the analytical techniques in the LIT database was assessed through a three-way Analysis of Variance (ANOVA) using the OGE classification scheme, the analytical techniques and LOI as categorical variables. The ANOVA design was unbalanced due to the unequal number of observations resulting from the level combinations of each factor (OGE, LOI and analytical techniques). Given an unbalanced design, the differences between the geochemical analysis techniques were assessed by pairwise comparisons of the Least square (LS) means calculated with the three-way ANOVA (the LS mean is an estimate of the population mean, gained from grouped data by adjusting for the influence of grouping, thereby adjusted for the imbalance of the ANOVA design). If the results of the pairwise comparison of the LS means show an agreement of the LS means between the different geochemical analysis techniques, the compiled database can be considered consistent within itself, thus, reliable. Data showing strong deviations from normality were transformed through the Box-Cox transformation (Zar, 2010).

b) Accuracy of the LIT database

One objective of the study is to evaluate whether the LIT database is accurate in the sense that mean geochemical concentrations per geological unit are representative for the units. Representativeness means that the frequency distribution of concentrations in samples is equal the true, but unknown one; in particular, the sample mean must be equal to the true mean. Deviation is called bias or inaccuracy. Since the true distributions

are not known, accuracy of samples cannot be validated by comparing sample and true distributions. However, a necessary – though not sufficient – condition for accuracy is that for each geological unit mean $TGDR_{calc}$ is equal (up to permitted tolerance) to mean $TGDR_{obs}$ in the same unit, taken from the RMP.

As a first step, the arithmetic mean of the $TGDR_{obs}$ for each geological unit studied of the OGE classification scheme (Table 1 and Figure 1) was estimated. The zonal statistics tool in ArcGis 10.5.1 (ESRI, Redland CA, USA, 2017) was used for this purpose. Given that the RMP data corresponds to data modelled by linear interpolation, due to the absence of outliers, the arithmetic mean is a robust measure of central tendency. Since the $TGDR$ per pixel of the RMP are given as class values, i.e. belonging to a class “i”, $TGDR \in (x_i, x_{i+1})$, the AM cannot be simply calculated from pixel values. This would be the straight-forward way, but the means per pixel are not available. An approximation is the weighted mean of class means, $(x_{i-1}+x_i)/2$, with weight the number of pixels $N(i-1, i)$ in this class divided by the total number of pixels, N . x_0 is set equal zero, which is the physically possible lower bound of a geochemical concentration. The question is how to deal with the highest class, labeled “ $>x_n$ ”, as no class mean can be calculated, since its upper bound is not known. This can be done approximately by assuming a tentative analytical model of the upper tail of the $TGDR$ distribution and calculate its contribution to the AM analytically. The maximum $TGDR_{obs}$ was estimated by polynomial regression of the $TGDR$ values displayed in the legend of the RMP (Batista et al. 2013). Polynomials of degree 6 and 7 were applied to maximize the multiple R-squared and minimize the residual standard error. A maximum $TGDR_{obs}$ of 236.911 nGy/h and 238.358 nGy/h were predicted from the 6-degree and 7-degree polynomial regression model fittings, respectively. The mean value of 237.6 nGy/h was set as the maximum $TGDR_{obs}$ in order to estimate the arithmetic means of $TGDR_{obs}$ for each geological unit. We tried two additional tail models, but the results are very similar and these models are not further discussed here.

As second step, the comparison of the arithmetic means between the LIT database and the RMP for each geological unit was carried out using the Student's paired sample t-test, the Wilcoxon median test and Pearson's correlation coefficient. The distributions of $TGDR_{calc}$ and $TGDR_{obs}$ were compared with the Anderson-Darling and Kolmogorov-Smirnov tests. Statistical analyses were performed with Statistica 7.0 (StatSoft Inc., USA) and R (Lenth, 2016; R Core Team, 2017).

3. Results and discussion

3.1. Analysis of the influence of the analytical techniques on LIT database

a) Effect size

The results of a three-away ANOVA performed on Box-Cox transformed data using the OGE classification scheme, LOI and the analytical techniques as categorical variables are shown in Table 3. The differences between the mean values of the analytical techniques and geological factors were significant at a 0.001 level of significance for U, Th, K and $TGDR_{calc}$. The effects of LOI were not significant at a 0.01 level of significance for U, Th, K and $TGDR_{calc}$.

The percentage of variation explained by the analytical techniques and LOI given by the partial eta-squared was close to or lower than 2 %, being lower than the variance explained by geological factors. According to Cohen's (1977) rule of thumb, the size of the effects of the analytical techniques and particularly LOI can be considered small (< 2 %) while the size of the effects of the geological factors was large (> 14 %). The variance explained by the LOI effects was generally lower than the variance explained by the analytical techniques (Table 3). The size of the effects of the analytical techniques was higher for the $TGDR_{calc}$ compared to the individual radioelements which is likely due to the combination of analytical techniques that results in a higher number of categories, hence, in a higher variability of geochemical analysis techniques used (Table 3).

The percentage of variation explained by geological factors was on average 53 % for U, 38 % for Th, 50% for K and 51 % for the $TGDR_{calc}$. The variance explained by

geological factors was much higher than the variance explained by the analytical techniques and LOI (Table 3). The geological factors are thereby the main source of variability in the data, followed by the error component. The latter can be assumed to mainly represent true spatial variability of geochemical concentrations – and in consequence the calculated dose rate $TGDR_{calc}$ – within geological units.

Table 3. Summary table of a three-way ANOVA performed on U, Th, K and $TGDR_{calc}$ Box-Cox transformed data using the OGE classification, LOI and the analytical techniques as categorical variables.

		SS	df	MS	F	p	Partial eta-squared (%)
U	OGE	2009.7	25	80.4	95.7	<0.001	52.7
	LOI	5.4	1	5.4	6.5	0.011	0.3
	Analytical techniques	33.0	2	16.5	19.7	<0.001	1.8
	Error	1801.1	2144	0.8			
Th	OGE	3457.9	26	133.0	58.70	<0.001	37.6
	LOI	0.9	1	0.9	0.38	0.536	<0.1
	Analytical techniques	37.9	2	18.9	8.35	<0.001	0.7
	Error	5741.2	2534	2.3			
K	OGE	1909.4	26	73.4	106.8	<0.001	50.4
	LOI	0.7	1	0.7	1.0	0.306	<0.1
	Analytical techniques	21.9	5	4.4	6.4	<0.001	1.2
	Error	1880.5	2735	0.7			
$TGDR_{calc}$	OGE	37380	25	1495	83.1	<0.001	50.7
	LOI	40	1	40	2.2	0.137	0.1
	Analytical techniques ^a	1882	9 ^a	209	11.6	<0.001	4.9
	Error	36311	2018	18			

SS – Sum of squares; df – degrees of freedom; MS – Mean square; F – F-test; p – p-value.

^aThe effects of the group where U and Th were determined by NAA and K by AAS are not estimable for the $TGDR_{calc}$, thus were excluded from the analysis.

b) Component effects

The differences between the LS means of the analytical techniques were investigated in Figure 2. The results of the pairwise comparison of the LS means are presented as supplementary material for U, Th and K (Table A3) and $TGDR_{calc}$ (Table A4). The ICP-MS LS mean was lower than the NAA and XRF means for both U and Th (Figure 2). For U, the LS means for NAA and XRF were 35 % higher, on average, than the ICP-MS mean. For Th, the XRF LS mean was 8 % higher while the NAA LS mean was 20 %

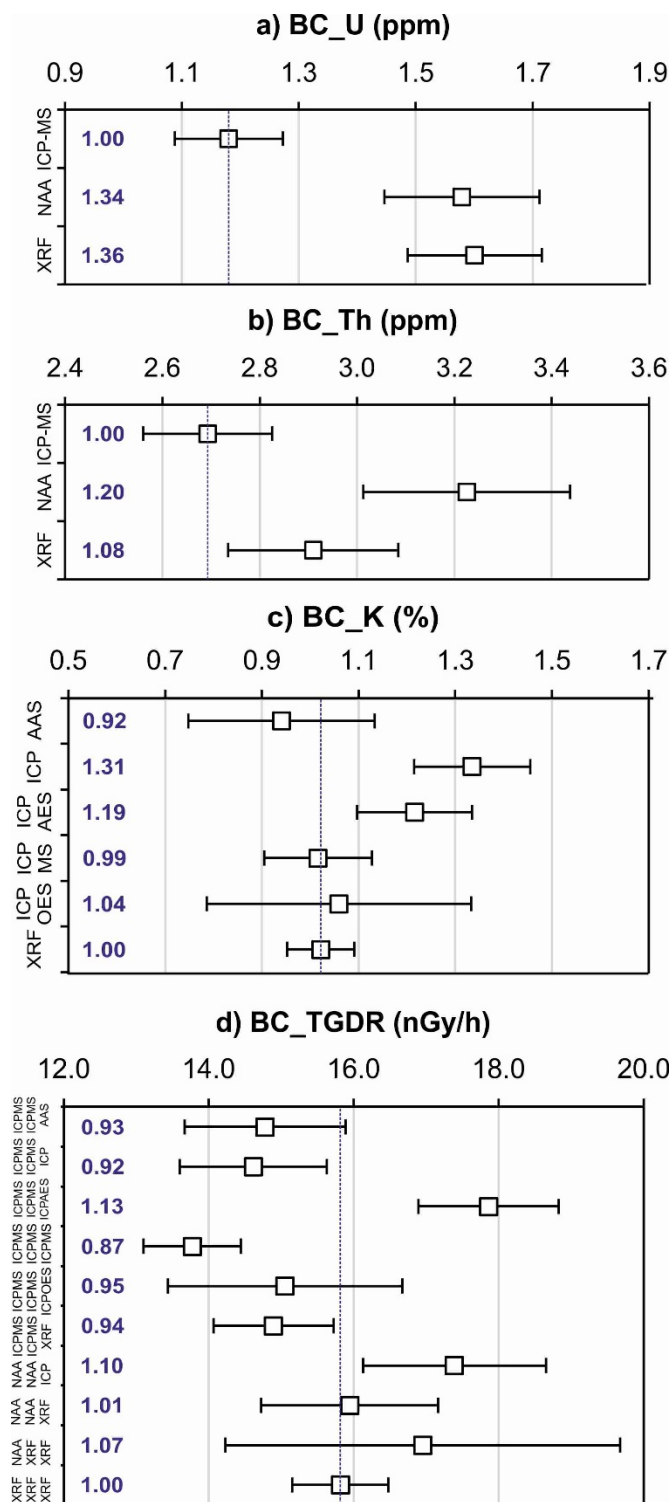
higher than the ICP-MS mean. The pairwise comparison of the LS means showed a systematic statistically significant differences between the ICP-MS data compared to other datasets (NAA and XRF) for U (Table A3). For Th, a statistically significant difference was observed between NAA and ICP-MS datasets, however, the differences between XRF and NAA, and XRF and ICP-MS were not significant (Table A3).

The analytical technique used to determine U was identical to the analytical technique used to determine Th (ICP-MS, NAA or XRF in 2084 out of the 2173 observations available for U (96% of the available data). As the ICP-MS LS means were generally lower for both elements, a significant bias of this analytical technique is suggested. The bias could be due to (1) a preference of the authors for analyzing rock samples with lower U and Th concentrations with the ICP-MS technique; (2) lower detection limits achieved by ICP-MS compared to other analytical techniques (e.g. Gill, 1997) or (3) by the technique limitations such as an inefficient digestion of typically resistant U- and Th-bearing minerals (e.g. zircon) or selective coprecipitation of these elements with fluorides when hydrofluoric acid is used in the digestion process (Preusser and Kasper, 2001).

For K, the pairwise comparison of the LS means indicated a general agreement between datasets apart from the observed statistically significant differences of the LS means where K was determined by the ICP technique (Table A3). These results are congruent with the observed LS mean of the ICP analysis technique which was 30 % higher than the reference mean chosen (XRF, see Figure 2). Given that only 8 out of 2768 observations present a K concentration below the LLD, it is unlikely that the observed difference could be caused by LLD values. Given that the ICP results were retrieved from older literature sources (ex. Mitjavila et al. 1997; Ribeiro 1998; Table A1) and that the ICP LS mean was higher than the reference mean chosen, the observed difference could be due to lack of reporting of values below the LLD by the authors. Apart from ICP and ICP-AES, deviations of the LS means from the reference mean chosen were generally lower than 10 %.

The results of the pairwise comparison of the LS means for $TGDR_{calc}$ showed a general agreement of the LS means between different geochemical analysis techniques (Table A4). Statistically significant differences between the LS means were only observed in 6 out of the 45 pairwise comparisons performed (Table A4). The compiled database can thus be considered consistent within itself, hence reliable. Apart from the dataset where K was determined by ICP-AES and ICP-MS, deviations of the LS means from the reference mean chosen are equal to or lower than 10 %. The LS means where U and Th data were acquired with ICP-MS are systematically lower than the LS means where U and Th data were acquired with NAA and XRF, which is consistent with the results observed for U and Th individually and can thus be caused by error propagation.

The LS means for the OGE units and LOI are presented as supplementary material (Figures A1 and A2). The LS means display large differences between the various OGE units for U, Th, K and $TGDR_{calc}$ (Figure A1), which are in accordance with the high percentage of variation explained by the OGE classification system (Table 3). With respect to LOI, higher LS means were expected in data corrected for the LOI and/or volatile content (corresponding to effect named "FALSE"), as are observed for K and the $TGDR_{calc}$ (Figure A2). However, lower LS means in LOI corrected data compared to uncorrected data are observed for U and Th (Figure A2 in Supplementary material). These results support the lack of a systematic influence of LOI. Given that the effects of LOI are not significant for U, Th and K (Table 3), it can be concluded that the correction of U, Th and K data for LOI or lack thereof does not affect significantly the results.



421

422 **Figure 2.** Plots of the least squares (LS) means of the analytical techniques effect for U,
 423 Th, K and TGDR_{calc} Box-Cox transformed data. The bars indicate the 95% confidence
 424 interval of the LS mean. A LS mean was chosen as reference for comparison according
 425 to higher sample size and number of geological units sampled (see Tables A1 and A2,
 426 supplementary material). The proportion of the LS means were calculated assuming the
 427 ICP-MS mean as reference for U and Th; the XRF mean for K and the dataset where U,
 428 Th and K were determined by XRF for the TGDR_{calc}.

3.2. Variance component originating from spatial variability

In the previous analysis, variance has been attributed entirely to geology (component A, see section 1.4) and analytical techniques (B), while component C was ignored, i.e. possible lack of representativeness of data for a geological unit. A possible procedure for resolving this would be performing an even higher stage ANOVA including individual data sources (each consisting of a number of data) as additional classification variable, or as simplification, simple ANOVA for data sources within individual geological units and for same analytical technique. However, data are not sufficient for this.

The sources of the error terms in Table 3 are measurement uncertainty and probably dominantly, spatial variability within units. Its contribution to the SS (sum of squares) is in the same order of magnitude as the one due to OGE. Given the data situation, it is however difficult to say to which degree possibly unrepresentative samples from the variable population contribute to bias of the mean. The question deserves further investigation in the future.

3.3. Comparison of the LIT and RMP datasets

The arithmetic means of the $TGDR_{calc}$ from U, Th and K compiled data were compared to the $TGDR_{obs}$ for each geological unit in Figure 3 and Table 4. The correlation between $TGDR_{calc}$ and $TGDR_{obs}$ was highly significant ($p < 0.001$). The results of a paired sample t-test and Wilcoxon median tests indicate that the differences between the arithmetic means of $TGDR_{calc}$ and $TGDR_{obs}$ were not statistically significant ($p = 0.126$ and $p = 0.14$, respectively). Distributions of $TGDR_{calc}$ and $TGDR_{obs}$ were about equal according to Kolmogorov-Smirnov and Anderson-Darling tests. If deviation from $TGDR_{obs}$ by pooled standard deviation (SD) is taken as criterion, 14 out of 26 OGE units are located within one pooled SD around $TGDR_{obs}$ (dashed lines in Figure 3), only 1 out of 26 is located outside 2 pooled SDs.

(The pooled SD is defined as

$$s_{pooled} = \sqrt{\frac{(n_1 - 1)s_1^2 + (n_2 - 1)s_2^2 + \dots + (n_k - 1)s_k^2}{n_1 + n_2 + \dots + n_k - k}} \quad (2)$$

with s_i the individual SDs and n_i the number of data in OGE unit (i). Its value is 29 nGy/h.)

A systematic overestimation of the $TGDR_{calc}$ compared to $TGDR_{obs}$ was observed for the sedimentary rocks (N2, N1c, K1-2, K1, TJ1 and the C2 units) coupled with absolute differences of the $TGDR_{calc}$ generally higher than 29 nGy/h (the pooled SD of the RMP dataset; Table 4, Figure 3). This effect may be caused, by (1) the lack of spatial representativeness of the data (as sampling of stratigraphic sequences is commonly carried out along vertical profiles instead of spatial grids) or (2) the lack of data from carbonate rocks. Carbonate rocks are a common subordinate lithology of the abovementioned geological units (see Table 1), presenting average radionuclides concentrations generally lower than siliciclastic rocks (e.g. Sêco et al. 2016).

Table 4. Comparison of the arithmetic means (\pm standard deviation) of the TGDR between LIT ($TGDR_{calc}$) and the RMP datasets ($TGDR_{obs}$).

Group	OGE unit	$TGDR_{calc}$ [1]	$TGDR_{obs}$ [2]	Difference [2] – [1]
Sedimentary rocks	N2	78 \pm 26	32 \pm 19	-46
	N1c	70 \pm 23	36 \pm 22	-34
	K1-2	106 \pm 21	42 \pm 28	-63
	K1	73 \pm 21 ^b	46 \pm 21	-27
	TJ1	85 \pm 29	44 \pm 20	-41
	C2	94 \pm 15	59 \pm 34	-35
Metamorphic rocks	C1-2	78 \pm 27 ^b	65 \pm 14	-13
	SDof	71 \pm 18	19 \pm 13	-52
	SD	39 \pm 41	90 \pm 22	51
	SDP	107 \pm 37 ^b	91 \pm 21	-16
	ODP	81 \pm 58 ^b	104 \pm 34	23
	O_a	69 \pm 38 ^b	88 \pm 27	18
	gz	77 \pm 25 ^b	87 \pm 28	10
	Npep	82 \pm 23 ^b	80 \pm 29	-2
	NP2	46 \pm 30 ^b	60 \pm 21	14
	NP1	31 \pm 31 ^b	56 \pm 29	25
Igneous rocks	gama2	68 \pm 35 ^b	63 \pm 16	-4
	CVL	52 \pm 23	14 \pm 10	-38
	g1_b	194 \pm 101 ^b	157 \pm 39	-37
	g2_b	137 \pm 59 ^b	172 \pm 40	35

	g3	157 ± 52 ^b	142 ± 46	-15
	g1_a	157 ± 88 ^b	136 ± 32	-21
	g2_a	150 ± 49 ^b	121 ± 24	-29
	g1a	61 ± 34 ^b	62 ± 23	1
	gama	9 ± 10	51 ± 19	43
	D3C1	50 ± 40 ^b	75 ± 26	25
^a TGDR _{obs} was calculated assuming an arbitrary maximum TGDR _{obs} of 237.6 nGy/h.				
^b The TGDR _{calc} is located within one pooled SD of the TGDR _{obs} .				

The arithmetic means of the TGDR_{calc} of granitic rocks are also generally overestimated in LIT database (g1_b, g3, g1_a and g2_a). In this case, the limitations of the RMP data must be taken into account, namely the fact that the maximum TGDR_{obs} in mainland Portugal is unknown. A value of 237.6 nGy/h was set as the maximum TGDR_{obs} in order to compute the mean TGDR_{obs} by geological unit. This issue only affects the geological units which display a TGDR_{obs} higher than 216.2 nGy/h, which are listed in Table 5 and include the abovementioned granitic rocks (g1_b, g2_b, g3, and g1_a). These units present a high percentage of their area (> 3 %) characterized by a TGDR_{obs} above 216.2 nGy/h. The underestimation of TGDR_{obs} of these units may be caused by the underestimation of the maximum TGDR_{obs} chosen (of 237.6 nGy/h), biasing the estimation mean TGDR_{obs} by geological unit.

Table 5. Percentage of the area characterized by a TGDR_{obs} higher than 216.2 nGy/h.

	OGE units	% of Area
Sedimentary rocks	N2	0.01
	N1c	0.05
	K1_2	0.68
	ODP	1.20
Metamorphic rocks	O_a	0.16
	gz	0.06
	NPep	0.47
	g1_b	5.36
Igneous rocks	g2_b	15.15
	g3	9.54
	g1_a	3.04
	g2_a	0.37

From a health perspective, the overestimation of the TGDR_{calc} is not as concerning as its underestimation, which was observed systematically in the SD, g2_b and the gama units. In the case of the g2_b unit, the difference observed between the TGDR_{calc} for

Model 1 is, however allocated within one SD of the $TGDR_{obs}$. The underestimation of the $TGDR_{calc}$ of the g2_b may be due to the underrepresentation of quantitative data from metallogenic deposits of uranium and/or radium that are common in the g2_b unit (ex. Marques et al. 2010; Neiva et al. 1987; Trindade et al. 2013). Because the g2_b dataset corresponds to one of the largest datasets available (Table A1, Supplementary material), this enforces the hypothesis that the major source of error within the compiled database was the insufficient representativeness of the data, which leads to a biased estimate of the mean, rather than the amount of data or the analytical techniques. Apart from the SD and SDof units, the absolute deviations between the arithmetic means of $TGDR_{calc}$ and $TGDR_{obs}$ were generally lower than 29 nGy/h for the metamorphic rocks (Table 4). For the SD unit, the only dataset available was retrieved from Dahn et al. (2014) and refers to mafic rocks outcropping in the SD unit. Thus, the underestimation of the $TGDR_{calc}$ reflects the lack of data from other types of rocks within the unit, particularly of the predominant lithology of the unit namely phyllites (Table 1). The underestimation of the $TGDR_{calc}$ of the gama unit may be due to the lack of data from differentiated rocks, such as anorthositic rocks and diorites (the subordinate lithologies of the gama unit, Table 1) that may present higher contents of terrestrial radionuclides than gabbros as U, Th and K become enriched with magmatic differentiation (Heier and Rogers, 1963).

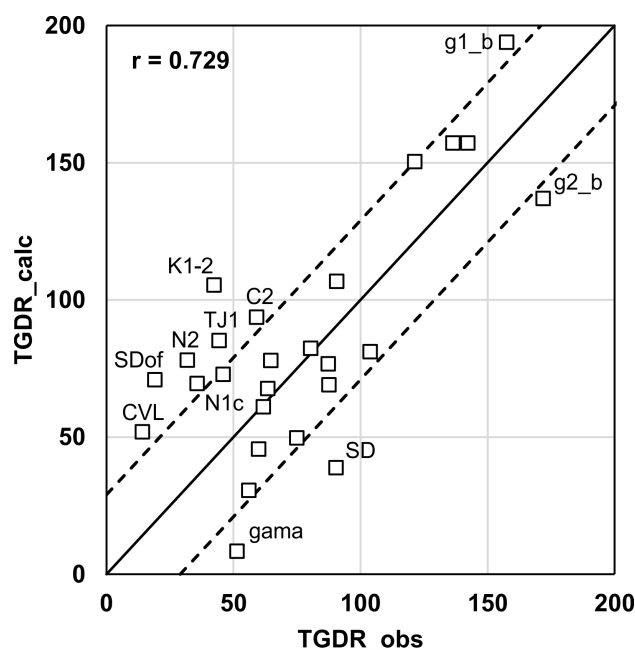


Figure 3. Scatterplot of the arithmetic means of the TGDR (in nGy/h) of each geological unit. The dashed lines indicate deviations of 29 nGy/h (the pooled SD) from the identity line.

The pooled SD of the RMP dataset was set as criterion to appraise the discrepancy between the arithmetic means of the RMP and LIT databases. Given the statistical parameters of the differences between $TGDR_{calc}$ and $TGDR_{obs}$ and their distributions, the compatibility of the RMP and LIT databases can be considered acceptable, but not perfect. For some geological units, the exact reason for discrepancy remains to be investigated, in order to improve further attempts of the kind.

As the $TGDR_{calc}$ was calculated from U, Th and K data compiled from scientific literature, the compatibility of the TGDR between the LIT and the RMP datasets (namely, $TGDR_{calc}$ and $TGDR_{obs}$) implies that the estimation of the contents of the terrestrial radionuclides in bedrock from compiled datasets is also reasonable. Putting it more precisely, since the approximate equality of $TGDR_{calc}$ and $TGDR_{obs}$ is only a necessary condition for the hypothesis to be true that the LIT database represents U, Th and K concentration in rocks reasonably well, the result of this investigation does not reject the hypothesis.

Vein-type rocks were excluded from the comparison exercise of LIT and RMP databases due to their large perimeter to area ratio. Given the compatibility of the RMP and LIT datasets, the $TGDR_{calc}$ of vein-type rocks was estimated resorting to data compiled from local geochemical surveys. The mean $TGDR_{calc}$ for the f1 and f2 (basic veins) and qz (quartz veins) units are presented in Table 6. The $TGDR_{calc}$ of basic vein-type rocks (f1 and f2) is similar to other mafic rocks units (ex. CVL, gama, and SDof units, Tables 1 and 4) as expected. Quartz veins present a similar $TGDR_{calc}$ to sedimentary and metamorphic rocks, being lower than the average $TGDR_{calc}$ of granitic rocks (Tables 1 and 4).

Table 6. Estimation of the TGDR of vein-type units using LIT data.

	OGE units	Number of samples	TGDR _{calc} (nGy/h)		References
			Mean	Standard deviation	
Vein-type rocks	f1	26	14	5	Cebriá et al. (2003); Martins (1999); Martins et al. (2009); Youbi et al. (2003);
	f2	17	34	14	Trindade et al. (2013); Alves (2010);
	qz	16	83	20	Lima (2000)

4. Conclusions

Two databases were compared with the aim of validating the compilation of literature data to estimate the mean concentrations of terrestrial radionuclides in bedrock using geological units as reference units. The results show that the compatibility of the databases was essentially reasonable. The differences between the arithmetic means were generally lower than the maximum allowable discrepancy set and the differences between the two databases were not statistically significant. A systematic overestimation of the contents of radionuclides calculated from the compiled data and observed in sedimentary rocks probably reflects the lack of representativeness of the data compiled for these units, while the differences observed for some granitic rocks may reflect the limitations of the TGDR_{obs}. Despite the significance of the effects of the analytical techniques, the variance explained by them, ranging from less than 1% to 5%, is sufficiently low, thereby lacking a significant impact on the comparability of the results acquired with different analytical techniques. The major sources of variability in the data are geological factors as demonstrated by the high percentage of variation explained by this factor in the ANOVA computed, as well as the true spatial variability of geochemical concentrations within geological units.

Geochemical characterization of geological units based on scattered literature data, as attempted in this study, allows the development of maps of terrestrial radionuclides contents in bedrock without large-scale sampling efforts, since a large amount of data is already available. Where extensive TGDR surveys are available, validation may be repeated e.g. along the lines presented here.

While the estimates computed for some units may be unreliable, they also set the groundwork needed to support further research. Certainly, a key problem is representativeness of the data, on which depends the reliability of the estimates of the mean contents of U, Th and K per geological units. It can be improved when more data with better coverage of geological units are available. Nonetheless, we think that generation of maps of U, Th and K concentrations in rock based on geological units is feasible.

Acknowledgements

The work was partly financed by the R&D Project ReNature (C2020-01-0145-FEDER-000007).

5. References

- Aires S., Carvalho C., Noronha F., Ramos J. F., Moura A. C., Sant'Ovaia H., and Sousa M. (2011) Os xistos do "Complexo Xisto-Grauváquico-Grupo do Douro": potencial como recurso geológico. In: *VI Seminário Recursos Geológicos, Ambiente e Ordenamento do Território*, 159-165.
- Alves C. A. S. F. (2010) Estudo petrológico e geoquímico do magmatismo transicional na Bacia Lusitânica. M.Sc. thesis. Lisboa Univ., pp. 134.
- Antunes A., Santos J. F., Azevedo M. R. Mendes M. H., and Ribeiro S. (2010) New petrographic, geochemical and geochronological data for the Reguengos de Monsaraz pluton (Ossa Morena Zone, SW Iberian Massif, Portugal). *Estud. Geol-Madrid*, **66**, 25-34. <http://dx.doi.org/10.3989/egeol.40162.123>.
- Antunes I. M. H. R. (2006) Mineralogia, Petrologia e Geoquímica de Rochas Granitóides da Área de Castelo Branco-Idanha-a-Nova. Ph.D. thesis. Coimbra Univ., pp. 482.
- Antunes I. M. H. R., Neiva A. M. R. Silva, M. M. V. G., and Corfu, F. (2009) The genesis of I-and S-type granitoid rocks of the Early Ordovician Oledo pluton, Central Iberian Zone (central Portugal). *Lithos*, **111**, 168-185. <https://doi.org/10.1016/j.lithos.2008.07.014>.

579 Antunes I. M. H. R., Neiva A. M. R., Ramos J. M. F., Silva P. B., Silva M. M. V. G., and
580 Corfu F. (2013) Petrogenetic links between lepidolite-subtype aplite-pegmatite, aplite
581 veins and associated granites at Segura (central Portugal). *Chem. Erde-Geochem.*,
582 **73**, 323-341. <https://doi.org/10.1016/j.chemer.2012.12.003>.

583 Antunes I. M. H. R., Neiva A. M. R., Silva M. M. V. G., and Corfu, F. (2008) Geochemistry
584 of S-type granitic rocks from the reversely zoned Castelo Branco pluton (Central
585 Portugal). *Lithos*, **103**, 445-465. <https://doi.org/10.1016/j.lithos.2007.10.003>.

586 Appleton, J. D., Miles, J. C. H., Green, B. M. R., and Larmour, R. (2008) Pilot study of
587 the application of Tellus airborne radiometric and soil geochemical data for radon
588 mapping. *J. Environ. Radioactiv.*, **99**, 1687-1697.

589 Arribas J., Tsige M., Garzón G., and Tejero R. (2014) Transport-Limited Denudation
590 Regime Inferred from Sand Petrography and Chemical Composition: Cenozoic
591 Sediments from the Guadiana Basin (SW Spain). *Int. J. Geoc.*, **5**, 478-496.
592 <http://dx.doi.org/10.4236/ijg.2014.55046>.

593 Baker G. R., and Jackson I. (2010) OneGeology-Europe, Final Report ECP-2001-GEO-
594 317001 (www.onegeologyeurope.org).

595 Batista, M. J., Prazeres, C., de Oliveira, D., and Leote, J. (2012) Radiometric Map of
596 Portugal. *In* Workshop on Recent developments in evaluation of uranium and thorium
597 resources.

598 Batista M. J., Torres L., Leote J., Prazeres C., Saraiva J., and Carvalho J. (2013) Carta
599 Radiométrica de Portugal (1:500 000). Laboratório Nacional de Energia e Geologia.
600 ISBN:978-989-675-027-5.

601 Beamish, D. (2014) Environmental radioactivity in the UK: the airborne geophysical view
602 of dose rate estimates. *J. Environ. Radioactiv.*, **138**, 249-263.

603 Boulter C. A., Hopkinson L. J., Ineson M. G., and Brockwell J. S. (2004) Provenance and
604 geochemistry of sedimentary components in the Volcano-Sedimentary Complex,

605 Iberian Pyrite Belt: discrimination between the sill-sediment-complex and volcanic-
 606 pile models. *J. Geol. Soc.*, **161**, 103-115. <https://doi.org/10.1144/0016-764902-159>.

607 Bustillo M., Pérez-Jiménez J. L., and Bustillo M. (2012) Caracterización geoquímica de
 608 rocas sedimentarias formadas por silicificación como fuentes de suministro de
 609 utensilios líticos (Mioceno, cuenca de Madrid). *Rev. Mex. Cienc. Geol.*, **29**, 233-247.

610 Caldeira, R., Ribeiro, M. L., and Moreira, M. E. (2007). Geoquímica das sequências
 611 máficas e félsicas entre Alvito, Torrão e Alcáçovas (SW da ZOM). *Comun. Geol.*, 94,
 612 5-28

613 Candeias C., Ávila P. F., da Silva E. F., and Teixeira J. P. (2015) Integrated approach to
 614 assess the environmental impact of mining activities: estimation of the spatial
 615 distribution of soil contamination (Panasqueira mining area, Central Portugal).
 616 *Environ. Monit. Assess.*, **187**, 135. <https://doi.org/10.1007/s10661-015-4343-7>.

617 Carvalho P. C. S., Neiva A. M. R., Silva M. M. V. G., and Corfu F. (2012) A unique
 618 sequential melting mechanism for the generation of anatectic granitic rocks from the
 619 Penafiel area, northern Portugal. *Lithos*, **155**, 110-124.
 620 <https://doi.org/10.1016/j.lithos.2012.08.019>.

621 Cebriá J. M., López-Ruiz J., Doblas M., Martins L. T., and Munhá J. (2003) Geochemistry
 622 of the early Jurassic Messejana–Plasencia dyke (Portugal–Spain); implications on the
 623 origin of the Central Atlantic Magmatic Province. *J. Petrol.*, **44**, 547-568.

624 Cerejo, T. A. R. (2013) Geoquímica da área de São Pedro das Águias – Concessão de
 625 Tabuaço. M.Sc. thesis, Aveiro Univ., pp. 153.

626 Cinelli, G., Tollefsen, T., Bossew, P., Gruber, V., Bogucarskis, K., de Felice, L., de Cort,
 627 M. (2019) Digital version of the European Atlas of natural radiation. *J. Environ.*
 628 *Radioact.* 196, 240–252.

629 Coelho F. M., Gomes M. E. P., and Neves L. J. P. F. (2007) Geochemistry of granites
630 and metasediments of the Vila Real region: implications for radon potential. In: Actas
631 do VI Congresso Ibérico de Geoquímica e XV Semana de Geoquímica, 65-68.

632 Cohen J. (1977) *Statistical power analysis for the behavioural sciences*. Academic Press,
633 pp. 490.

634 Costa M. M. C. P. (2006) Geoquímica de granitóides de Pera Velha-Vila Nova de Paiva-
635 Ferreira de Aves. M.Sc. thesis, Aveiro Univ, pp. 179.

636 Costa M. M. C. P. (2011) Geoquímica dos granitoides de Aguiar da Beira, Norte de
637 Portugal. Ph.D. thesis, Aveiro Univ., pp. 365.

638 Costa M. M., Neiva A. M. R., Azevedo M. R., and Corfu F. (2014) Distinct sources for
639 syntectonic Variscan granitoids: Insights from the Aguiar da Beira region, Central
640 Portugal. *Lithos*, **196**, 83-98. <https://doi.org/10.1016/j.lithos.2014.02.023>.

641 Crumbling D. M. (2001) In Search Of Representativeness: Evolving the Environmental
642 Data Quality Model. *Qual. Assur.*, **9**, 179-190.

643 Cruz A. R. Z. S. (2007) Relações Petrogeoquímicas dos Maciços Graníticos do NE
644 Alentejano. Ph.D. thesis, Coimbra Univ., pp. 404.

645 Dahn D. R., Braid J. A., Murphy J. B., Quesada C., Dupuis N., and McFarlane C. R.
646 (2014) Geochemistry of the Peramora Mélange and Pulo do Lobo schist: geochemical
647 investigation and tectonic interpretation of mafic mélange in the Pangean suture zone,
648 Southern Iberia. *Int. J. Earth Sci.*, **103**, 1415-1431. [https://doi.org/10.1007/s00531-](https://doi.org/10.1007/s00531-014-1024-7)
649 [014-1024-7](https://doi.org/10.1007/s00531-014-1024-7).

650 Darnley, A. G. (1995) International Geochemical mapping – a review. *J. Geochem.*
651 *Explor.*, **55**, 5-10.

652 Darnley, A. G., Bjorklund, A., Bolviken, B., Gustavsson, N., Koval, P. V., Steenfelt, A.,
653 Tauchid, M., and Xuejing, X. (1995) A Global geochemical database.

654 Recommendations for international geochemical mapping. Final report of IGCP
655 project, 259, UNESCO Publishing.

656 Dias P. S. A. (2011) Análise estrutural e paragenética de produtos litológicos e
657 mineralizações de segregação metamórfica: estudo de veios hiperaluminosos e
658 protólitos poligénicos silúricos da região da Serra de Arga (Minho). Ph.D. thesis,
659 Minho Univ., pp. 615.

660 Dinis P., and Oliveira Á. (2016) Provenance of Pliocene clay deposits from the Iberian
661 Atlantic Margin and compositional changes during recycling. *Sediment. Geol.*, **336**,
662 171-182. <https://doi.org/10.1016/j.sedgeo.2015.12.011>.

663 Dinis P. A., Dinis J. L., Mendes M. M., Rey J., and Pais, J. (2016) Geochemistry and
664 mineralogy of the Lower Cretaceous of the Lusitanian Basin (western Portugal):
665 Deciphering palaeoclimates from weathering indices and integrated vegetational
666 data. *C. R. Geosci.*, **348**, 139-149.

667 Dinis P. A., Oliveira Á., Rocha F., Vieira M., and Cunha P. P. (2011) Evolution in the
668 provenance of a tectonically controlled Plio–Pleistocene alluvial system between the
669 Variscan Iberian Massif and the Atlantic margin, Portugal. *Chem. Erde-Geochem.*,
670 **71**, 267-278. <https://doi.org/10.1016/j.chemer.2010.12.001>.

671 European Commission (EC), 2019. European Atlas of Natural Radiation. In: De Cort, M.
672 G., Tollefsen, T. (Eds.). Publication Office of the European Union, Joint Research
673 Centre – Cinelli, Luxembourg, ISBN 978-92-76-08259-0. [https://doi.org/10.2760/](https://doi.org/10.2760/520053)
674 520053. Catalogue number KJ-02-19-425-EN-C, EUR 19425 EN.

675 ESRI, 2017. ArcGIS version 10.5.1. Environmental Systems Resource Institute,
676 Redlands, CA.

677 Ferreira J. A. S. (2013) Caracterização do granito do Pedregal. Condicionantes da sua
678 aplicação. Ph.D. thesis, Porto Univ., pp. 155.

679 Fuenlabrada J. M., Arenas R., Fernández R. D., Martínez S. S., Abati J., and Carmona
680 A. L. (2012) Sm–Nd isotope geochemistry and tectonic setting of the
681 metasedimentary rocks from the basal allochthonous units of NW Iberia (Variscan
682 suture, Galicia). *Lithos*, **148**, 196-208. <https://doi.org/10.1016/j.lithos.2012.06.002>.

683 Fuenlabrada J. M., Arenas R., Martínez S. S., García F. D., and Castiñeiras P. (2010) A
684 peri-Gondwanan arc in NW Iberia: I: isotopic and geochemical constraints on the
685 origin of the arc – a sedimentary approach. *Gondwana Res.*, **17**, 338-351.
686 <https://doi.org/10.1016/j.gr.2009.09.007>.

687 Fuenlabrada J. M., Pieren A. P., Fernández R. D., Martínez S. S., and Arenas R. (2016)
688 Geochemistry of the Ediacaran–Early Cambrian transition in Central Iberia: Tectonic
689 setting and isotopic sources. *Tectonophysics*, **681**, 15-30.
690 <https://doi.org/10.1016/j.tecto.2015.11.013>.

691 Gill, R. (1997). Modern analytical geochemistry: An introduction to quantitative chemical
692 analysis techniques for earth, environmental and materials scientists. London:
693 Longman.

694 Godinho M. M., Pereira A. J. S. C., and Neves L. J. P. F. (1986) Análise geoquímica
695 comparada dos plutonitos de Caramulo, Avô e Zebreira (Portugal Central). *Memórias
696 e Notícias*, **102**, 43-68.

697 Godinho M. M., Pereira A. J. S. C., and Neves, L. J. P. F. (1991) Potencial térmico das
698 rochas graníticas num segmento do Maciço Hespérico (Portugal Central). *Memórias
699 e Notícias*, **112**, 469-483.

700 Gomes M. E. P. (1989) Geoquímica dos granitóides e seus minerais da região de
701 Telões-Vilarinho da Samardã. M.Sc. thesis, Aveiro Univ. pp. 173.

702 Gomes M. E. P. (2008) Geochemistry of microgranular enclaves and host granite from
703 Telões (Vila Pouca de Aguiar), Northern Portugal. *Chem. Erde-Geochem.*, **68**, 69-80.
704 <https://doi.org/10.1016/j.chemer.2005.08.001>.

- Gomes M. E. P., Martins L. M. O., Neves L. J. P. F., and Pereira A. J. C. S. (2013) Natural radiation and geochemical data for rocks and soils, in the North International Douro Cliffs (NE Portugal). *J. Geochem. Explor.*, **130**, 60-64. <https://doi.org/10.1016/j.gexplo.2013.03.001>.
- Gomes M. E. P., and Neiva A. M. R. (2005) Geochemistry of granitoids and their minerals from Rebordelo–Agrochão area, northern Portugal. *Lithos*, **81**, 235-254. <https://doi.org/10.1016/j.lithos.2004.11.001>.
- Gomes M. E. P., and Neiva A. M. R. (2002) Petrogenesis of tin-bearing granites from Ervedosa, northern Portugal: the importance of magmatic processes. *Chem. Erde-Geochem.*, **62**, 47-72. <https://doi.org/10.1078/0009-2819-00002>.
- Gomes M. E. P., Neves L. J. P. F., Coelho F., Carvalho A., Sousa M., and Pereira A. J. S. C. (2011) Geochemistry of granites and metasediments of the urban area of Vila Real (northern Portugal) and correlative radon risk. *Environ. Earth Sci.*, **64**, 497-502. <https://doi.org/10.1007/s12665-010-0873-z>.
- Gómez-Pugnaire M. T., Azor A., Fernández-Soler J. M., and Sánchez-Vizcaino V. L. (2003) The amphibolites from the Ossa–Morena/Central Iberian Variscan suture (Southwestern Iberian Massif): geochemistry and tectonic interpretation. *Lithos*, **68**, 23-42. [https://doi.org/10.1016/S0024-4937\(03\)00018-5](https://doi.org/10.1016/S0024-4937(03)00018-5).
- Grange M., Scharer U., Merle R., Girardeau J., and Cornen G. (2010) Plume–lithosphere interaction during migration of Cretaceous alkaline magmatism in SW Portugal: evidence from U–Pb ages and Pb–Sr–Hf isotopes. *J. Petrol.*, **51**, 1-28. <https://doi.org/10.1093/petrology/egq018>.
- Grasty, R. L., Tauchid, M., and Torres, L. M. M. (1993) Standardization of old gamma ray survey data. In Application of uranium exploration data and techniques in environmental studies. Proceedings of a Technical Committee meeting IAEA-TECDOC-827, Vienna, 9-12 November.

731 Heier, S. H., and Rogers, J. J. W. (1963) Radiometric determination of thorium, uranium
 732 and potassium in basalts and in two magmatic differentiation series. *Geochim.*
 733 *Cosmochim. Acta*, 27(2), 137-154.

734 Henriques S. B. A., Neiva A. M. R., and Dunning G. R. (2016) Petrogenesis of a late-
 735 Variscan rhyodacite at the Ossa Morena-Central Iberian zones boundary, Iberian
 736 Massif, Central Portugal: Evidence for the involvement of lithospheric mantle and
 737 meta-igneous lower crust. *Chem. Erde-Geochem.*, **76**, 429-439.
 738 <https://doi.org/10.1016/j.chemer.2016.06.003>.

739 Henriques S. B. A., Neiva A. M. R., Tajčmanová L., and Dunning G. R. (2017) Cadomian
 740 magmatism and metamorphism at the Ossa Morena/Central Iberian zone boundary,
 741 Iberian Massif, Central Portugal: Geochemistry and P–T constraints of the Sardoal
 742 Complex. *Lithos*, **268**, 131-148. <https://doi.org/10.1016/j.lithos.2016.11.002>.

743 Henriques S., Ribeiro M. L., and Moreira M. E. (2006) Caracterização petrográfica e
 744 geoquímica dos magmatitos da região do Sardoal (Abrantes) e seu enquadramento
 745 geodinâmico. *Comun. Geol.*, **93**, 5-22.

746 IAEA (International Atomic Energy Agency) (2010) *Radioelement mapping* (series no.
 747 NF-T-1.3). International Atomic Energy Agency, Vienna, pp. 123.

748 Ielsch, G., Cuney, M., Buscail, F., Rossi, F., Leon, A., and Cushing, M. E. (2017)
 749 Estimation and mapping of uranium content of geological units in France. *J. Environ.*
 750 *Radioactiv.*, **166**, 210-219.

751 Ielsch, G., Cushing, M. E., Combes, P., and Cuney, M. (2010) Mapping of the geogenic
 752 radon potential in France to improve radon risk management: methodology and first
 753 application to region Bourgogne. *J. Environ. Radioactiv.*, **101**, 813-820.

754 Jaques L., Noronha F., Liewig N., and Bobos I. (2016) Paleofluids circulation associated
 755 with the Gerês late-orogenic granitic massif, northern Portugal. *Chem. Erde-Geochem.*, **76**, 659-676. <https://doi.org/10.1016/j.chemer.2016.09.006>.

757 Jesus, A. P., Mateus, A., Munhá, J. M., and Tassinari, C. (2014). Internal architecture
 758 and Fe–Ti–V oxide ore genesis in a Variscan synorogenic layered mafic intrusion, the
 759 Beja Layered Gabbroic Sequence (Portugal). *Lithos*, 190, 111-136.

760 Jesus A. P., Mateus A., Munhá J. M., Tassinari C. C., dos Santos T. M. B., and Benoit
 761 M. (2016) Evidence for underplating in the genesis of the Variscan synorogenic Beja
 762 Layered Gabbroic Sequence (Portugal) and related mesocratic rocks.
 763 *Tectonophysics*, **683**, 148-171. <https://doi.org/10.1016/j.tecto.2016.06.001>.

764 Jorge R. C. G. S., Fernandes P., Rodrigues B., Pereira Z., and Oliveira J. T. (2013)
 765 Geochemistry and provenance of the Carboniferous Baixo Alentejo Flysch Group,
 766 South Portuguese Zone. *Sediment. Geol.*, **284**, 133-148.
 767 <https://doi.org/10.1016/j.sedgeo.2012.12.005>.

768 Lenth, R. V. (2016) Least-Squares Means: The {R} Package {lsmeans}. *J. Stat. Softw.*,
 769 **69**, 1-33.

770 Lima A. M. C. (2000) Estrutura, Mineralogia e Génese dos Filões Aplitopegmatíticos com
 771 Espodumena da Região Barroso-Alvão. Ph.D. thesis, Porto Univ. and Institut National
 772 Polytechnique de Lorraine, pp. 300.

773 Lima S. M., Neiva A. M. R., and Ramos J. M. F. (2013) Adakitic-like magmatism in
 774 western Ossa-Morena Zone (Portugal): Geochemical and isotopic constraints of the
 775 Pavia pluton. *Lithos*, **160-161**, 98-116. <https://doi.org/10.1016/j.lithos.2012.11.020>.

776 Lima S. M., Neiva A. M., Ramos J. M., and Cuesta A. (2014) Long-lived magmatic
 777 systems and implications on the recognition of granite–pegmatite genetic relations:
 778 Characterization of the Pavia granitic pegmatites (Ossa-Morena Zone, Portugal).
 779 *Chem. Erde-Geochem.*, **74**, 625-639. <https://doi.org/10.1016/j.chemer.2014.02.003>.

780 Lisboa J. V., Oliveira D. P. S., Rocha F., Oliveira A., and Carvalho J. (2015) Patterns of
 781 rare earth and other trace elements in Paleogene and Miocene clayey sediments from

782 the Mondego platform (Central Portugal). *Chem. Erde-Geochem.*, **75**, 389-401.
 783 <https://doi.org/10.1016/j.chemer.2015.07.002>.

784 LNEG (Laboratório Nacional de Energia e Geologia) (2010) Carta Geológica de Portugal
 785 à escala 1:1 000 000. Laboratório Nacional de Energia e Geologia, Unidade de
 786 Geologia, Hidrogeologia e Geologia Costeira.

787 Lorda M. S., Sarrionandia F., Ábalos B., Carracedo M., Eguíluz L., and Ibarguchi J. G.
 788 (2013) Geochemistry and paleotectonic setting of Ediacaran metabasites from the
 789 Ossa-Morena Zone (SW Iberia). *Int. J. Earth Sci.*, **103**, 1263-1286.
 790 <https://doi.org/10.1007/s00531-013-0937-x>.

791 Marques R., Jorge A., Franco D., Dias M. I., and Prudêncio M. I. (2010) Clay resources
 792 in the Nelas region (Beira Alta), Portugal. A contribution to the characterization of
 793 potential raw materials for prehistoric ceramic production. *Clay Miner.*, **45**, 353-370.
 794 <https://doi.org/10.1180/claymin.2010.045.3.353>.

795 Marsac, K. E., Burnley, P. C., Adcock, C. T., Haber, D. A., Malchow, R. L., and Hausrath,
 796 E. M. (2016) Modeling background radiation using geochemical data: A case study in
 797 and around Cameron, Arizona. *J. Environ. Radioactiv.*, **165**, 68-85.

798 Martins H. C. B., Sant'Ovaia H., and Noronha F. (2009) Genesis and emplacement of
 799 felsic Variscan plutons within a deep crustal lineation, the Penacova-Régua-Verín
 800 fault: an integrated geophysics and geochemical study (NW Iberian Peninsula).
 801 *Lithos*, **111**, 142-155. <https://doi.org/10.1016/j.lithos.2008.10.018>.

802 Martins H. C. B., Sant'Ovaia H., and Noronha F. (2013) Late-Variscan emplacement and
 803 genesis of the Vieira do Minho composite pluton, Central Iberian Zone: Constraints
 804 from U–Pb zircon geochronology, AMS data and Sr–Nd–O isotope geochemistry.
 805 *Lithos*, **162-163**, 221-235. <https://doi.org/10.1016/j.lithos.2013.01.001>.

806 Martins, L. T. (1999) Cretaceous Alkaline Magmatism in Algarve Littoral (South
 807 Portugal): a Basanite-Lamprophyre Rock Suite. *GeoLines*, **9**, 84-91.

808 Miranda R. M. L. (2010) Petrogenesis and Geochronology of the Late Cretaceous
809 Alkaline Magmatism in the West Iberian Margin. Ph.D. thesis, Lisboa Univ., pp. 488.

810 Miranda R., Valadares V., Terrinha P., Mata J., Azevedo M. R., Gaspar M., Kullberg J.
811 C., and Ribeiro C. (2009) Age constraints on the Late Cretaceous alkaline magmatism
812 on the West Iberian Margin. *Cretaceous Res.*, **30**, 575-586.
813 <https://doi.org/10.1016/j.cretres.2008.11.002>.

814 Mitjavila J., Martí J., and Soriano C. (1997) Magmatic evolution and tectonic setting of
815 the Iberian Pyrite Belt volcanism. *J. Petrol.*, **38**, 727-755.
816 <https://doi.org/10.1093/petroj/38.6.727>.

817 Moita, P., Santos, J. F., and Pereira, M. F. (2009) Layered granitoids: interaction
818 between continental crust recycling processes and mantle-derived magmatism:
819 examples from the Évora Massif (Ossa–Morena Zone, southwest Iberia, Portugal).
820 *Lithos*, **111**, 125-141. <https://doi.org/10.1016/j.lithos.2009.02.009>.

821 Neiva A. M. R. (1993) Geochemistry of Granites and their Minerals from Gerez Mountain,
822 Northern Portugal. *Chem. Erde-Geochem.*, **53**, 227-258.

823 Neiva A. M. R., and Gomes M. E. P. (1991) Geochemistry of the granitoid rocks and their
824 minerals from Lixa do Alvão-Alfarela de Jales-Tourencinho (Vila Pouca de Aguiar,
825 northern Portugal). *Chem. Geol.*, **89**, 305-327. [https://doi.org/10.1016/0009-2541\(91\)90022-J](https://doi.org/10.1016/0009-2541(91)90022-J).

826

827 Neiva A. M. R., Silva P. B., Corfu F., and Ramos J. M. F. (2011a) Sequential melting and
828 fractional crystallization: Granites from Guarda-Sabugal area, central Portugal. *Chem.*
829 *Erde-Geochem.*, **71**, 227-245. <https://doi.org/10.1016/j.chemer.2011.06.002>.

830 Neiva A. M. R., Silva P. B., and Ramos J. M. (2011b) Geochemistry of granitic aplite-
831 pegmatite veins and sills and their minerals from the Sabugal area, central Portugal.
832 *Neues Jb. Miner. Abh.*, **189**, 49-74. <https://dx.doi.org/10.1127/0077-7757/2011/0209>.

833 Neiva A. M. R., Williams I. S., Ramos J. M. F., Gomes M. E. P., Silva M. M. V. G., and
834 Antunes I. M. H. R. (2009) Geochemical and isotopic constraints on the petrogenesis
835 of Early Ordovician granodiorite and Variscan two-mica granites from the Gouveia
836 area, central Portugal. *Lithos*, **111**, 186-202.
837 <https://doi.org/10.1016/j.lithos.2009.01.005>.

838 Neiva A. M., Gomes M. E., Ramos J. M., and Silva P. B. (2008) Geochemistry of granitic
839 aplite-pegmatite sills and their minerals from Arcozelo da Serra area (Gouveia, central
840 Portugal). *Eur. J. Mineral.*, **20**, 465-485. [https://dx.doi.org/10.1127/0935-](https://dx.doi.org/10.1127/0935-1221/2008/0020-1827)
841 [1221/2008/0020-1827](https://dx.doi.org/10.1127/0935-1221/2008/0020-1827).

842 Neiva A. M. R., Neiva J. M. C., and Parry, S. J. (1987) Geochemistry of the granitic rocks
843 and their minerals from Serra da Estrela, Central Portugal. *Geochim. Cosmochim.*
844 *Acta*, **51**, 439-454. [https://doi.org/10.1016/0016-7037\(87\)90060-3](https://doi.org/10.1016/0016-7037(87)90060-3).

845 Neves L. J. P. F., and Pereira, A. J. S. C. (2007) Alguns dados geoquímicos e
846 radiométricos sobre o granodiorito de Chãs (Vila Nova de Foz Côa, Portugal Central).
847 In: VI Congresso Ibérico de Geoquímica e XV Semana de Geoquímica, 141-145.

848 Neves L. J. P. F., Pereira L. C., Pereira A. J. S. C., Stephens W. E., and Godinho M. M.
849 (1998) Scorzalite-bearing granitic rocks of the Pedrógrão Grande pluton (Central
850 Portugal): mineralogical and geochemical characterization. *Acta U. C. Geol.*, **42**, 83-
851 85.

852 Neves L. J. P. F., Stephens W. E., Pereira A. J. S. C., Godinho M. M., and Fallick A. E.
853 (1999) The São Pedro do Sul granite (Central Portugal): an HHP Th-rich rock of the
854 Hesperian Massif. *An. Acad. Bras. Cienc.*, **71**, 51-65.

855 Neves L., Pereira A., and Macedo C. (2007) Alguns dados geoquímicos e
856 geocronológicos (K-Ar) sobre o plutonito granítico de Tancos (Portugal Central). In:
857 VI Congresso Ibérico de Geoquímica e XV Semana de Geoquímica, 137-140.

858 Noronha F., Carvalho C., Aires S., Moura A. C., and Ramos J. F. (2012) "Schist" as a
 859 geological resource of "Trás-os-Montes e Alto Douro" (NE Portugal). In: Global Stone
 860 Congress.

861 Oliveira M. F. B. (2015) Controlos lito-estratigráficos, mineralógicos e geoquímicos da
 862 jazida de ferro da Carvalhosa (Serra do Reboredo, Torre de Moncorvo). Stage
 863 Report, Lisboa Univ., pp. 203.

864 Pedro J. M. C. (2004) Estudo geológico e geoquímico das Sequências Ofiolíticas
 865 Internas da Zona de Ossa-Morena (Portugal). Ph.D. thesis, Évora Univ., pp. 319.

866 Pereira M. F., Chichorro M., Linnemann U., Eguluz L., and Silva J. B. (2006) Inherited
 867 arc signature in Ediacaran and Early Cambrian basins of the Ossa-Morena zone
 868 (Iberian Massif, Portugal): paleogeographic link with European and North African
 869 Cadomian correlatives. *Precambrian Res.*, **144**, 297-315.
 870 <https://doi.org/10.1016/j.precamres.2005.11.011>.

871 Pereira M. F., Chichorro M., Solá A. R., Silva J. B., Sánchez-García T., and Bellido F.
 872 (2011) Tracing the Cadomian magmatism with detrital/inherited zircon ages by in-situ
 873 U–Pb SHRIMP geochronology (Ossa-Morena Zone, SW Iberian Massif). *Lithos*, **123**,
 874 204-217. <https://doi.org/10.1016/j.lithos.2010.11.008>.

875 Pinto F. M. V. (2014) Estudo da distribuição do Estanho na Mina da Panasqueira. M.Sc.
 876 thesis, Porto Univ., pp. 236.

877 Preusser, F., and Kasper, H. U. (2001) Comparison of dose rate determination using
 878 high-resolution gamma spectrometry and inductively coupled plasma – mass
 879 spectrometry. *Ancient TL*, **19**, 19-23.

880 Quesada C., Fonseca P. E., Munha J., Oliveira J. T., and Ribeiro A. (1994) The Beja-
 881 Acebuches Ophiolite (Southern Iberia Variscan fold belt): Geological characterization
 882 and geodynamic significance. *B. Geol. Min.*, **105**, 3-49.

883 R Core Team (2017) R: A language and environment for statistical computing. R
 884 Foundation for Statistical Computing, Vienna, Austria. URL <http://www.R-project.org/>.

885 Ramírez J. A., and Grundvig S. (2000) Causes of geochemical diversity in peraluminous
 886 granitic plutons: the Jalama pluton, Central-Iberian Zone (Spain and Portugal). *Lithos*,
 887 **50**, 171-190. [https://doi.org/10.1016/S0024-4937\(99\)00047-X](https://doi.org/10.1016/S0024-4937(99)00047-X).

888 Ramírez J. A., and Menéndez L. G. (1999) A geochemical study of two peraluminous
 889 granites from south-central Iberia: the Nisa-Albuquerque and Jalama batholiths.
 890 *Mineral. Mag.*, **63**, 85-104. <https://doi.org/10.1180/002646199548330>.

891 Reis M., Freitas M. C., Dung H. M., Mateus A., Paiva I., Madruga M. J., Gonçalves M.
 892 A., Silva L., and Dionísio I. (2012) Characterization of geomaterials from NE Portugal
 893 using k_0 -based instrumental neutron activation analysis (k_0 -INAA) and gamma
 894 spectrometry methods. *J. Radioanal. Nucl. Ch.*, **294**, 363-369.
 895 <https://doi.org/10.1007/s10967-012-1613-5>.

896 Ribeiro J., da Silva E. F., Li Z., Ward C., and Flores D. (2010) Petrographic, mineralogical
 897 and geochemical characterization of the Serrinha coal waste pile (Douro Coalfield,
 898 Portugal) and the potential environmental impacts on soil, sediments and surface
 899 waters. *Int. J. Coal Geol.*, **83**, 456-466. <https://doi.org/10.1016/j.coal.2010.06.006>.

900 Ribeiro M. A. (1998) Estudo litogeoquímico das formações metassedimentares
 901 encaixantes de mineralizações em Trás-os-Montes Ocidental. Implicações
 902 Metalogenéticas. Ph.D. thesis. Porto Univ.

903 Rollinson, H. R. (1993) Using geochemical data: evaluation, presentation, interpretation.
 904 Harlow, Essex, England: New York: Longman Scientific & Technical, 352 pp.

905 Rosa D. R. N., Inverno C. M. C., Oliveira V. M. J., and Rosa C. J. P. (2006) Geochemistry
 906 and geothermometry of volcanic rocks from Serra Branca, Iberian Pyrite Belt,
 907 Portugal. *Gondwana Res.*, **10**, 328-339. <https://doi.org/10.1016/j.gr.2006.03.008>.

- Rosa D. R. N., Inverno C. M. C., Oliveira V. M. J., and Rosa C. J. P. (2004) Geochemistry of volcanic rocks, Albernoa area, Iberian pyrite belt, Portugal. *Int. Geol. Rev.*, **46**, 366-383. <http://dx.doi.org/10.2747/0020-6814.46.4.366>.
- Sánchez-García T., Bellido F., Pereira M. F., Chichorro M., Quesada C., Pin C., and Silva J. B. (2010) Rift-related volcanism predating the birth of the Rheic Ocean (Ossa-Morena zone, SW Iberia). *Gondwana Res.*, **17**, 392-407. <https://doi.org/10.1016/j.gr.2009.10.005>.
- Sánchez-García T., Pereira M. F., Bellido F., Chichorro M., Silva J. B., Valverde-Vaquero P., Pin C., and Solá A. R. (2013) Early Cambrian granitoids of North Gondwana margin in the transition from a convergent setting to intra-continental rifting (Ossa-Morena Zone, SW Iberia). *Int. J. Earth Sci.*, **103**, 1203-1218. <https://doi.org/10.1007/s00531-013-0939-8>.
- Saraiva, J. M., Torres, L. M. M., and Leote, J. (1998) Aplicações da cartografia radiométrica na protecção ambiental e na prospecção de recursos. Proceedings of the IX Assembleia Nacional de Geodesia y Geofísica, 9-13 February, Almeria, Spain.
- Schütz W., Ebner J., and Meyer K.-D. (1987) Trondhjemites, tonalites and diorites in the South Portuguese Zone and their relations to the vulcanites and mineral deposits of the Iberian Pyrite Belt. *Geol. Rundsch.*, **76**, 201-212. <https://doi.org/10.1007/BF01820583>.
- Sêco, S., Domingos, F., Pereira, A., and Duarte, L.V. (2016) Radon emanation of sedimentary rocks: a case study in the Lusitanian Basin (western Portugal). In 13th International Workshop on the Geological Aspects of Radon Risk Mapping, Prague.
- Silva M. A. (2014a) Petrogenesis of a variscan migmatite complex (NW Portugal): petrography, geochemistry and fluids. Ph.D. thesis, Porto Univ., pp. 456.

932 Silva P. J. A. B. A. (2014b) Mineralogia, petrologia e geoquímica de granitos e filões
 933 aplito-pegmatíticos da região de Guarda-Sabugal. Ph.D. thesis. Trás-os-Montes e
 934 Alto Douro Univ.

935 Silva P. J. A. B. A. (2000) Estudo petrográfico, mineralógico e geoquímico dos maciços
 936 graníticos de Bruçó e Fonte Santa. M.Sc. thesis, Porto Univ., pp. 210.

937 Silva S. I. P. F. (2007) Estudo geoquímico de metabasitos da ZOM e da ZCI aflorantes
 938 na região Centro-Norte de Portugal. M.Sc. thesis, Aveiro Univ., pp. 217.

939 Silva M. M. V. G., and Neiva A. M. R. (1990) Geochemistry of the granites and their
 940 minerals from Paredes da Beira-Penedono, northern Portugal. *Chem. Geol.*, **85**, 147-
 941 170. [https://doi.org/10.1016/0009-2541\(90\)90128-T](https://doi.org/10.1016/0009-2541(90)90128-T).

942 Silva M. M. V. G., Neiva A. M. R., and Whitehouse M. J. (2000) Geochemistry of enclaves
 943 and host granites from the Nelas area, central Portugal. *Lithos*, **50**, 153-170.
 944 [https://doi.org/10.1016/S0024-4937\(99\)00053-5](https://doi.org/10.1016/S0024-4937(99)00053-5).

945 StatSoft Inc., 2004. STATISTICA (data analysis software system), version 7. 1009
 946 www.statsoft.com.

947 Tauchid, M., and Grasty, R. L. (2002). Natural background radioactivity of the earth's
 948 surface--essential information for environmental impact studies, IAEA, IAEA-SM-
 949 362/25, 230-242.

950 Teixeira R. J. S. (2008) Mineralogia, petrologia e geoquímica dos granitos e seus
 951 enclaves da região de Carrazeda de Ansiães. Ph.D. thesis, Trás-os-Montes e Alto
 952 Douro Univ., pp. 463.

953 Teixeira, R. J. S., Neiva, A. M. R., and Gomes, M. E. P. (2010). Geochemistry of
 954 amphibole asbestos from northeastern Portugal and its use in monitoring the
 955 environmental impact of asbestos from quarrying. *Comun. Geol.*, **97**, 99-112.

956 Teixeira R. J. S., Neiva A. M. R., Gomes M. E. P., Corfu F., Cuesta A., and Croudace I.
 957 W. (2012) The role of fractional crystallization in the genesis of early syn-D 3, tin-

958 mineralized Variscan two-mica granites from the Carrazeda de Ansiães area,
 959 northern Portugal. *Lithos*, **153**, 177-191. <https://doi.org/10.1016/j.lithos.2012.04.024>.

960 Torres, L. M., and Grasty, R. L. (1993) The Natural Radioactivity Map of Portugal. In
 961 Application of uranium exploration data and techniques in environmental studies.
 962 Proceedings of a Technical Committee meeting IAEA-TECDOC-827, Vienna, 9-12
 963 November.

964 Torres, L., Leote, J., and Silva, M. (1997) Carta de Radiação Gama Natural na escala
 965 1/200 000. Departamento de Geologia, Instituto Geológico e Mineiro, Lisboa.

966 Trindade M. J. F. (2007) Geoquímica e mineralogia de argilas da Bacia Algarvia:
 967 transformações térmicas. Ph.D. thesis, Aveiro Univ., pp. 459.

968 Trindade M. J., Rocha F., and Dias M. I. (2010) Geochemistry and mineralogy of clays
 969 from the Algarve Basin, Portugal: a multivariate approach to palaeoenvironmental
 970 investigations. *Curr. Anal. Chem.*, **6**, 43-52.
 971 <https://doi.org/10.2174/157341110790069682>.

972 Trindade M. J., Prudêncio M. I., Burbidge C. I., Dias M. I., Cardoso G., Marques R., and
 973 Rocha F. (2013) Distribution of naturally occurring radionuclides (K, Th and U) in
 974 weathered rocks of various lithological types from the uranium bearing region of
 975 Fornos de Algodres, Portugal. *Mediterranean Archaeol. Archaeom.*, **13**, 71-79.

976 Ugidos J. M., Armenteros I., Barba P., Valladares M. I., and Colmenero J. R. (1997a)
 977 Geochemistry and petrology of recycled orogen-derived sediments: a case study from
 978 Upper Precambrian siliciclastic rocks of the Central Iberian Zone, Iberian Massif,
 979 Spain. *Precambrian Res.*, **84**, 163-180. [https://doi.org/10.1016/S0301-](https://doi.org/10.1016/S0301-9268(97)00023-5)
 980 [9268\(97\)00023-5](https://doi.org/10.1016/S0301-9268(97)00023-5).

981 Ugidos J. M., Billström K., Valladares M. I., and Barba P. (2003a) Geochemistry of the
 982 Upper Neoproterozoic and Lower Cambrian siliciclastic rocks and U-Pb dating on

983 detrital zircons in the Central Iberian Zone, Spain. *Int. J. Earth Sci.*, **92**, 661-676.
 984 <https://doi.org/10.1007/s00531-003-0355-6>.

985 Ugidos J. M., Valladares M. I., Barba P., and Ellam R. M. (2003b) The Upper
 986 Neoproterozoic–Lower Cambrian of the Central Iberian Zone, Spain: chemical and
 987 isotopic (Sm-Nd) evidence that the sedimentary succession records an inverted
 988 stratigraphy of its source. *Geochim. Cosmochim. Acta*, **67**, 2615-2629.
 989 [https://doi.org/10.1016/S0016-7037\(03\)00027-9](https://doi.org/10.1016/S0016-7037(03)00027-9).

990 Ugidos J. M., Valladares M. I., Recio C., Rogers G., Fallick A. E., and Stephens W. E.
 991 (1997b) Provenance of Upper Precambrian-Lower Cambrian shales in the Central
 992 Iberian Zone, Spain: evidence from a chemical and isotopic study. *Chem. Geol.*, **136**,
 993 55-70. [https://doi.org/10.1016/S0009-2541\(96\)00138-6](https://doi.org/10.1016/S0009-2541(96)00138-6).

994 Ugidos J. M., Sánchez-Santos J. M., Barba P., and Valladares M. I. (2010) Upper
 995 Neoproterozoic series in the Central Iberian, Cantabrian and West Asturian Leonese
 996 Zones (Spain): geochemical data and statistical results as evidence for a shared
 997 homogenised source area. *Precamb. Res.*, **178**, 51-58.
 998 <https://doi.org/10.1016/j.precamres.2010.01.009>.

999 UNSCEAR (United Nations Scientific Committee on the Effects of Atomic Radiation)
 1000 (2010) Sources and effects of ionizing radiation. UNSCEAR 2008 Report to the
 1001 General Assembly with Scientific Annexes, vol. I, United Nations, pp. 683.

1002 Valladares M. I., Barba P., Ugidos J. M., Colmenero J. R., and Armenteros I. (2000)
 1003 Upper Neoproterozoic–Lower Cambrian sedimentary successions in the Central
 1004 Iberian Zone (Spain): sequence stratigraphy, petrology and chemostratigraphy.
 1005 Implications for other European zones. *Int. J. Earth Sci.*, **89**, 2-20.
 1006 <https://doi.org/10.1007/s005310050314>.

1007 Valladares M. I., Ugidos J. M., Barba P., and Colmenero J. R. (2002) Contrasting
 1008 geochemical features of the Central Iberian Zone shales (Iberian Massif, Spain):

1009 implications for the evolution of Neoproterozoic–Lower Cambrian sediments and their
 1010 sources in other peri-Gondwanan areas. *Tectonophysics*, **352**, 121-132.
 1011 [https://doi.org/10.1016/S0040-1951\(02\)00192-0](https://doi.org/10.1016/S0040-1951(02)00192-0).

1012 van der Weijden C. H., and van der Weijden R. D. (1995) Mobility of major, minor and
 1013 some redox-sensitive trace elements and rare-earth elements during weathering of
 1014 four granitoids in central Portugal. *Chem. Geol.*, **125**, 149-167.
 1015 [https://doi.org/10.1016/0009-2541\(95\)00071-S](https://doi.org/10.1016/0009-2541(95)00071-S).

1016 Villaseca C., Merino E., Oyarzun R., Orejana D., Pérez-Soba C., and Chicharro E. (2014)
 1017 Contrasting chemical and isotopic signatures from Neoproterozoic metasedimentary
 1018 rocks in the Central Iberian Zone (Spain) of pre-Variscan Europe: Implications for
 1019 terrane analysis and Early Ordovician magmatic belts. *Precambrian Res.*, **245**, 131-
 1020 145. <https://doi.org/10.1016/j.precamres.2014.02.006>.

1021 Youbi N., Martins L. T., Munha J. M., Ibouh H., Madeira J., Aït Chayeb E. H., and El
 1022 Boukhari A. (2003) The Late Triassic-Early Jurassic Volcanism of Morocco and
 1023 Portugal in the Framework of the Central Atlantic Magmatic Province: An Overview.
 1024 In: The Central Atlantic Magmatic Province: Insights from Fragments of Pangea (ed.
 1025 W. Hames), Geophys. Monogr. Ser., 136, 179-207.

1026 Xuejing, X., and Hangxin, C. (2001) Global geochemical mapping and its implementation
 1027 in the Asia–Pacific region. *Appl. Geochem.*, **16**(11-12), 1309-1321.

1028 Zar, J. H. (2010) Biostatistical Analysis, 5th Edition. Prentice-Hall, New Jersey, 944 pp.

1029 **Supplementary material**

1030 **Table A1.** Summary of the data available in LIT database for the OGE units sampled by
1031 geological unit. 2173 observations were compiled for U, 2564 for thorium and 2768 for K
1032 acquired with 7 different analytical techniques.

OGE unit	Analytical Technique ^a	N (U)	N (Th)	N (K)	References
C1-2	ICP-MS	74	74	0	Jorge et al. (2013); Trindade (2007)
	ICP-OES	0	0	74	
	NAA	7	7	0	
	XRF	0	0	7	
C2	ICP-MS	18	20	18	Dinis et al. (2011); Ribeiro et al. (2010)
	XRF	0	0	2	
CVL	ICP-MS	62	62	62	Miranda (2010); Miranda et al. (2009)
D2-3	XRF	0	30	32	Boulter et al. (2004)
D3C1	ICP	0	0	59	Boulter et al. (2004); Mitjavila et al. (1997); Rosa et al. (2004, 2006); Schützet al. (1987)
	NAA	59	129	0	
	XRF	28	27	135	
g1_a	AAS	0	0	17	Coelho et al. (2007); Costa et al. (2014); Ferreira (2013); Godinho et al. (1986, 1991); Gomes (1989); Gomes and Neiva (2002, 2005); Gomes et al. (2011, 2013); Neiva and Gomes, (1991); Neiva et al. (2008, 2009); Neves et al. (1999); Silva (2000, 2014a); Teixeira (2008); Teixeira et al. (2012)
	ICP	0	0	32	
	ICP-AES	0	0	7	
	ICP-MS	77	77	0	
	NAA	4	13	0	
	XRF	150	205	230	
g1_b	ICP-AES	0	0	15	Costa (2011); Costa et al. (2014); Gomes and Neiva (2005);
	ICP-MS	15	15	0	
	NAA	6	6	0	
	XRF	0	0	6	
g1a	ICP-AES	0	0	22	Antunes et al. (2010); Lima et al. (2013, 2014); Moita et al. (2009)
	ICP-MS	57	79	57	
g2_a	ICP-AES	0	0	12	Cerejo (2013); Neves et al. (2007); Silva and Neiva (1990)
	ICP-MS	12	12	0	
	NAA	10	10	0	
	XRF	8	8	18	
g2_b	AAS	0	0	43	Antunes (2006); Antunes et al. (2008, 2013); Carvalho et al. (2012); Costa (2006, 2011); Godinho et al. (1991); Lima et al. (2013, 2014); Marques et al. (2010); Martins et al. (2013); Neiva et al. (1987, 2009, 2011a, 2011b); Ramírez and Grundvig (2000); Silva (2014b); Silva et al. (2000); Trindade et al. (2013); van der Weijden and van der Weijden (1995)
	ICP-AES	0	0	134	
	ICP-MS	165	164	24	
	NAA	23	13	0	
	XRF	185	259	281	
g3	ICP-AES	0	0	64	Costa (2006, 2011); Gomes (2008); Jaques et
	ICP-MS	56	56	6	

OGE unit	Analytical Technique ^a	N (U)	N (Th)	N (K)	References
	NAA	0	3	0	al. (2016); Martins et al. (2009); Neiva (1993); Neves and Pereira, (2007); Ramirez and Menéndez (1999)
	XRF	14	14	32	
GAMA	ICP	0	0	60	Caldeira et al. (2007); Jesus et al. (2014, 2016); Pedro (2004); Quesada et al. (1994)
	ICP-MS	92	97	138	
	NAA	32	32	0	
	XRF	0	0	15	
GAMA2	ICP-MS	16	16	16	Grange et al. (2010); Miranda (2010)
gz	ICP-MS	8	8	4	Antunes (2006); Antunes et al. (2009); Cruz (2007); Godinho et al. (1986); Neves et al. (1998); Pereira et al. (2006, 2011); Sánchez-García et al. (2010, 2013)
	XRF	25	57	62	
K1	NAA	52	52	0	Trindade (2007); Trindade et al. (2010)
	XRF	0	0	52	
K1-2	ICP-MS	45	45	0	Dinis et al. (2016)
	XRF	0	0	45	
N1c	ICP	0	0	32	Arribas et al. (2014); Bustillo et al. (2012); Lisboa et al. (2015); Marques et al. (2010); Reis et al. (2012)
	ICP-AES	0	0	5	
	ICP-MS	48	48	0	
	NAA	16	16	0	
	XRF	0	0	16	
N2	ICP-MS	45	72	5	Dinis and Oliveira (2016); Dinis et al. (2011); Pereira et al. (2006); Trindade (2007)
	NAA	6	6	0	
	XRF	0	0	88	
NP1	ICP-AES	0	0	69	Gómez-Pugnaire et al. (2013); Henriques et al. (2017); Silva (2007)
	ICP-MS	90	90	0	
	XRF	0	0	21	
NP2	ICP	0	0	14	Dinis et al. (2011); Henriques et al. (2006, 2016); Lorda et al. (2013); Pereira et al. (2006, 2011)
	ICP-AES	0	0	5	
	ICP-MS	16	63	42	
	XRF	1	1	3	
Npep	AAS	0	0	16	Aires et al. (2011); Candeias et al. (2015); Cerejo (2013); Coelho et al. (2007); Dinis et al. (2011); Fuenlabrada et al. (2016); Godinho et al. (1991); Marques et al. (2010); Neves et al. (1999); Noronha et al. (2012); Oliveira (2015); Pinto (2014); Ribeiro (1998); Silva (2014a); Trindade et al. (2013); Ugidos et al. (1997a, 1997b, 2003a, 2003b, 2010); Valladares et al. (2000, 2002); Villaseca et al. (2014)
	ICP	0	0	35	
	ICP-AES	0	0	176	
	ICP-MS	310	341	86	
	ICP-OES	0	0	24	
	NAA	9	9	0	
	XRF	22	22	30	
O_a	ICP	0	0	1	Oliveira (2015); Pereira et al. (2011); Ribeiro et al. (2010); Silva (2014a)
	ICP-MS	2	2	1	
	XRF	15	15	15	
ODP	ICP	0	0	52	Dias (2011); Noronha et al. (2012); Ribeiro (1998)
	ICP-MS	41	41	0	
	NAA	46	46	0	
	XRF	6	6	47	
SD	XRF	33	33	33	Dahn et al. (2014)

OGE unit	Analytical Technique ^a	N (U)	N (Th)	N (K)	References
SDof	AAS	0	0	5	Fuenlabrada et al. (2010, 2012); Teixeira et al. (2010)
	ICP-MS	48	43	0	
	ICP-OES	0	0	43	
SDP	ICP	0	0	60	Noronha et al. (2012); Ribeiro (1998)
	NAA	54	55	0	
	XRF	3	3	3	
TJ1	NAA	62	62	0	Trindade (2007); Trindade et al. (2010)
	XRF	0	0	60	

N – number of observations.
^aICP-MS – Inductively Coupled Plasma Mass Spectrometry; ICP-OES – Inductively Coupled Plasma Optical Emission Spectrometry; NAA – Neutron Activation Analysis; XRF – X-Ray Fluorescence; ICP – Inductively Coupled Plasma; ICP-AES – Inductively Coupled Plasma Atomic Emission Spectrometry; AAS – Atomic Absorption Spectrometry.

1033

1034 **Table A2.** Summary of the data available by analytical technique.

	Analytical technique			Number of samples (N)	% N	Number of OGEs sampled	%OGE
	U	Th	K				
U	NAA			386	17.8	14	51.9
	XRF			490	22.5	12	44.4
	ICP-MS			1297	59.7	21	77.8
Th		NAA		459	17.9	15	55.6
		XRF		680	26.5	13	48.1
		ICP-MS		1425	55.6	21	77.8
K			AAS	81	2.9	4	14.8
			ICP-OES	141	5.1	3	11.1
			ICP-MS	459	16.6	12	44.4
			ICP	345	12.5	9	33.3
			ICP-AES	509	18.4	10	37.0
			XRF	1233	44.5	23	85.2
TGDR _{calc} ^a	ICP-MS	ICP-MS	ICP-MS	330	16.1	12	44.4
	ICP-MS	ICP-MS	ICP-OES	141	6.9	3	11.1
	ICP-MS	ICP-MS	ICP	143	7.0	5	18.5
	NAA	NAA	ICP	176	8.6	5	18.5
	NAA	NAA	XRF	160	7.8	8	29.6
	XRF	XRF	XRF	421	20.5	11	40.7
	ICP-MS	ICP-MS	XRF	217	10.6	10	37.0
	ICP-MS	ICP-MS	ICP-AES	380	18.5	8	29.6
	ICP-MS	ICP-MS	AAS	76	3.7	3	11.1
	NAA	XRF	XRF	10	0.5	1	3.7

^aThe analytical techniques listed for the TGDR_{calc} refer to the compilation of the analytical techniques used to analyse U, Th and K.

1035

Table A3. Pairwise comparison of the LS means of the analytical techniques for U, Th and K. P-values were adjusted with the false discovery rate (FDR) method (Lenth, 2016).

	Analytical techniques under comparison	Difference between the LS means	SE	t	p
U (df = 2144)	NAA x ICP-MS	-0.399	0.085	-4.691	<0.001(*)
	NAA x XRF	-0.022	0.091	-0.240	0.9688
	ICP-MS x XRF	-0.421	0.075	-5.589	<0.001(*)
Th (df = 2534)	NAA x ICP-MS	-0.532	0.132	-4.033	<0.001(*)
	NAA x XRF	0.316	0.145	2.171	0.076
	ICP-MS x XRF	-0.217	0.115	-1.890	0.142
K (df = 2735)	AAS x ICP	-0.394	0.116	-3.411	0.009(*)
	AAS x ICP-AES	-0.276	0.112	-2.469	0.134
	AAS x ICP-MS	-0.076	0.114	-0.667	0.986
	AAS x ICP-OES	-0.119	0.169	-0.708	0.981
	AAS x XRF	-0.081	0.099	-0.822	0.964
	ICP x ICP-AES	0.119	0.076	1.562	0.624
	ICP x ICP-MS	0.319	0.077	4.163	0.001(*)
	ICP x ICP-OES	0.275	0.155	1.770	0.485
	ICP x XRF	0.313	0.067	4.664	<0.001(*)
	ICP-AES x ICP-MS	0.200	0.075	2.674	0.081
	ICP-AES x ICP-OES	0.156	0.148	1.055	0.899
	ICP-AES x XRF	0.194	0.066	2.923	0.041
	ICP-MS x ICP-OES	-0.044	0.154	-0.282	1.000
	ICP-MS x XRF	-0.006	0.071	-0.078	1.000
	ICP-OES x XRF	0.038	0.151	0.253	1.000

SE – standard error; t, p – t-test and respective p-value. Significant values at $\alpha = 0.01$ are indicated with (*).

1039 **Table A4.** Pairwise comparison of the LS means of the analytical techniques for TGDR_{calc}
1040 (df = 2018). P-values were adjusted with the false discovery rate (FDR) method (Lenth,
1041 2016).

Analytical techniques ^a under comparison						Difference between the LS means	SE	t	p									
U	Th	K		U	Th	K												
ICP-MS	ICP-MS	AAS	x	ICP-MS	ICP-MS	ICP	0.162	0.780	0.208	1.000								
				ICP-MS	ICP-MS	ICP-AES	-3.082	0.761	-4.052	0.002(*)								
				ICP-MS	ICP-MS	ICP-MS	1.005	0.653	1.538	0.877								
				ICP-MS	ICP-MS	ICP-OES	-0.275	1.058	-0.260	1.000								
				ICP-MS	ICP-MS	XRF	-0.118	0.712	-0.166	1.000								
				NAA	NAA	ICP	-2.611	0.900	-2.902	0.106								
				NAA	NAA	XRF	-1.168	0.888	-1.316	0.950								
				NAA	XRF	XRF	-2.175	1.434	-1.517	0.886								
			XRF	XRF	XRF	-1.038	0.544	-1.907	0.664									
ICP-MS	ICP-MS	ICP	x	ICP-MS	ICP-MS	ICP-AES	-3.245	0.516	-6.289	<0.001(*)								
				ICP-MS	ICP-MS	ICP-MS	0.842	0.561	1.501	0.892								
				ICP-MS	ICP-MS	ICP-OES	-0.437	0.901	-0.485	1.000								
				ICP-MS	ICP-MS	XRF	-0.280	0.587	-0.478	1.000								
				NAA	NAA	ICP	-2.774	0.786	-3.530	0.015								
				NAA	NAA	XRF	-1.330	0.798	-1.668	0.814								
				NAA	XRF	XRF	-2.338	1.498	-1.560	0.867								
				XRF	XRF	XRF	-1.200	0.630	-1.906	0.665								
ICP-MS	ICP-MS	ICP-AES	x	ICP-MS	ICP-MS	ICP-MS	4.087	0.527	7.749	<0.001(*)								
				ICP-MS	ICP-MS	ICP-OES	2.807	0.828	3.392	0.025								
				ICP-MS	ICP-MS	XRF	2.964	0.545	5.439	<0.001(*)								
				NAA	NAA	ICP	0.471	0.778	0.606	1.000								
				NAA	NAA	XRF	1.914	0.782	2.448	0.298								
				NAA	XRF	XRF	0.907	1.482	0.612	1.000								
				XRF	XRF	XRF	2.045	0.616	3.318	0.031								
				ICP-MS	ICP-MS	ICP-MS		ICP-MS	ICP-MS	ICP-OES	-1.280	0.895	-1.429	0.918				
ICP-MS	ICP-MS	XRF	-1.123					0.555	-2.024	0.582								
NAA	NAA	ICP	-3.616					0.760	-4.759	<0.001(*)								
NAA	NAA	XRF	-2.173					0.751	-2.894	0.108								
NAA	XRF	XRF	-3.180					1.429	-2.225	0.440								
XRF	XRF	XRF	-2.042					0.492	-4.155	0.001(*)								
ICP-MS	ICP-MS	ICP-OES	x					ICP-MS	ICP-MS	XRF	0.157	0.932	0.168	1.000				
								NAA	NAA	ICP	-2.336	1.074	-2.176	0.474				
				NAA	NAA	XRF	-0.893	0.988	-0.903	0.996								
				NAA	XRF	XRF	-1.900	1.661	-1.144	0.980								
				XRF	XRF	XRF	-0.763	0.963	-0.792	0.999								
				ICP-MS	ICP-MS	XRF	x	NAA	NAA	ICP	-2.493	0.695	-3.586	0.013				
								NAA	NAA	XRF	-1.050	0.782	-1.343	0.944				
								NAA	XRF	XRF	-2.057	1.456	-1.413	0.924				
XRF	XRF	XRF	-0.920					0.542	-1.696	0.798								
NAA	NAA	ICP	x					NAA	NAA	XRF	1.443	0.944	1.528	0.881				
								NAA	XRF	XRF	0.436	1.558	0.280	1.000				
								XRF	XRF	XRF	1.574	0.769	2.047	0.566				
								NAA	NAA	XRF	x	NAA	XRF	XRF	-1.007	1.552	-0.649	1.000
				XRF	XRF	XRF	0.130					0.764	0.170	1.000				
				NAA	XRF	XRF	x					XRF	XRF	XRF	1.137	1.375	0.827	0.998

SE – standard error; t, p – t-test and respective p-value. Significant values at $\alpha = 0.01$ are indicated with (*). ^aThe analytical techniques listed for the TGDR_{calc} refer to the compilation of the analytical techniques used to analyse U, Th and K.

1042

1043 **Table B1.** Compiled geochemical database.

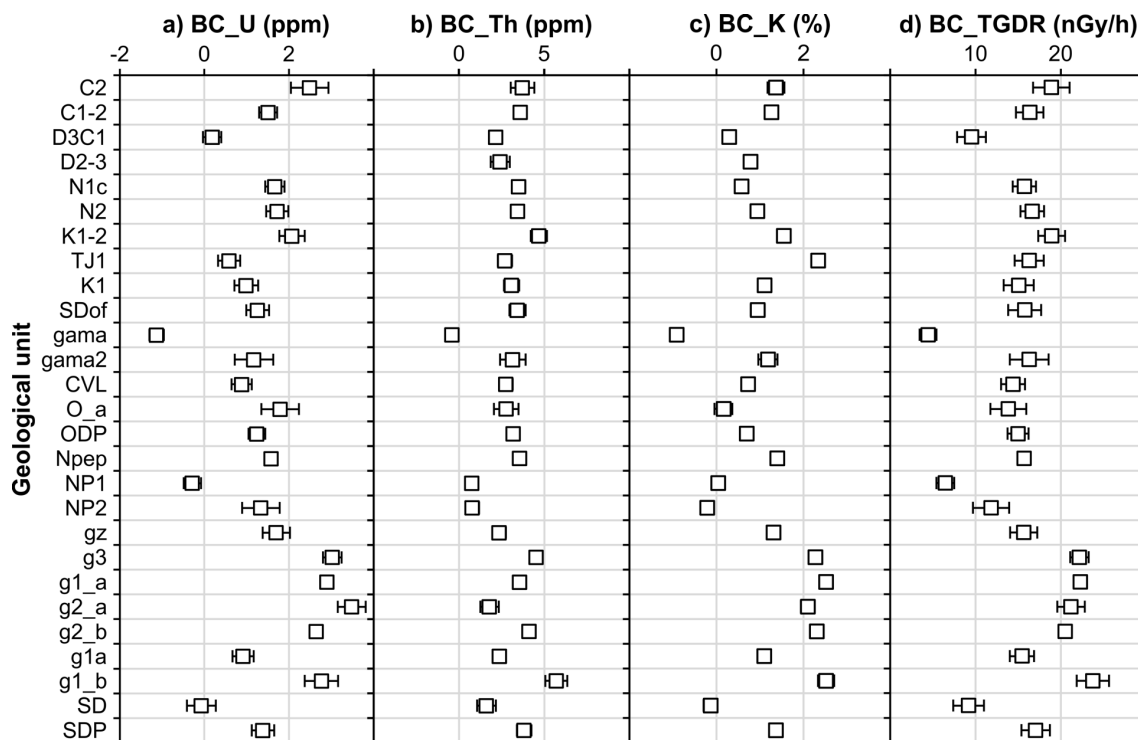


Figure A1. Plots of the least squares (LS) means of the OGE effect for U, Th, K and TGDR_{calc} Box-Cox (BC) transformed data by geological unit. The bars indicate the 95% confidence interval of the LS mean.

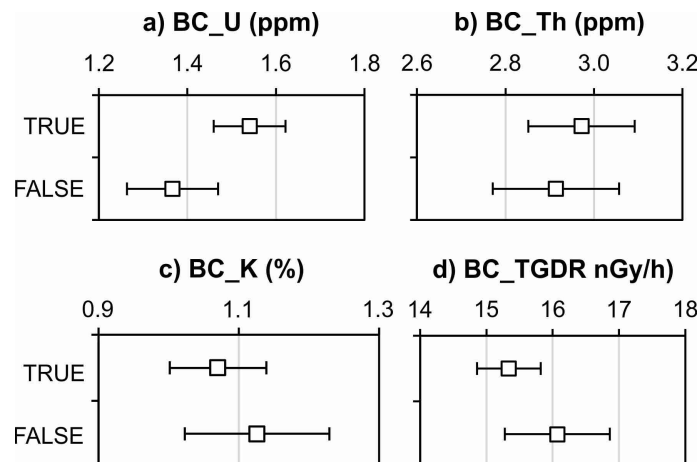


Figure A2. Plots of the least squares (LS) means of the LOI effect for U, Th, K and TGDR_{calc} Box-Cox (BC) transformed data. The bars indicate the 95% confidence interval of the LS mean. Each observation of U, Th, K and TGDR_{calc} is classified as “true” if the authors estimated but did not corrected the data for LOI (or the volatile content) and “false” otherwise.